© 2015. Published by The Company of Biologists Ltd | Development (2015) 142, 3943-3953 doi:10.1242/dev.129841

RESEARCH ARTICLE

Maternal BCAS2 protects genomic integrity in mouse early embryonic development

Qianhua Xu[1,2,*], Fengchao Wang[3,*], Yunlong Xiang[1], Xiaoxin Zhang[1], Zhen-Ao Zhao[1], Zheng Gao[1,2], Wenbo Liu[1], Xukun Lu[1,2], Yusheng Liu[1], Xing-Jiang Yu[1], Haibin Wang[1], Jun Huang[4], Zhaohong Yi[5], Shaorong Gao[6,‡] and Lei Li[1,‡]

ABSTRACT

Mammalian early embryos maintain accurate genome integrity for proper development within a programmed timeline despite constant assaults on their DNA by replication, DNA demethylation and genetic defects transmitted from germ cells. However, how genome integrity is safeguarded during mammalian early embryonic development remains unclear. BCAS2 (breast carcinoma amplified sequence 2), a core component of the PRP19 complex involved in pre-mRNA splicing, plays an important role in the DNA damage response through the RPA complex, a key regulator in the maintenance of genome integrity. Currently, the physiological role of BCAS2 in mammals is unknown. We now report that BCAS2 responds to endogenous and exogenous DNA damage in mouse zygotes. Maternal depletion of BCAS2 compromises the DNA damage response in early embryos, leading to developmental arrest at the two- to four-cell stage accompanied by the accumulation of damaged DNA and micronuclei. Furthermore, BCAS2 mutants that are unable to bind RPA1 fail in DNA repair during the zygotic stage. In addition, phosphorylated RPA2 cannot localise to the DNA damage sites in mouse zygotes with disrupted maternal BCAS2. These data suggest that BCAS2 might function through the RPA complex during DNA repair in zygotes. Together, our results reveal that maternal BCAS2 maintains the genome integrity of early embryos and is essential for female mouse fertility.

KEY WORDS: Maternal effect genes, Mouse early embryonic development, BCAS2, Genomic integrity, DNA damage

INTRODUCTION

Organisms and cells have evolved complex systems for responding to DNA damage to ensure the survival and faithful transmission of genetic materials to subsequent generations. Depending on the type of DNA lesion, cells generally arrest cell cycle progression by activating the DNA damage response (DDR), which includes sensing DNA lesions and triggering cascades mediated by the ATM (ataxia telangiectasia mutated) and ATR (ataxia telangiectasia and Rad3 related) kinases to repair damaged DNA (Ciccia and Elledge, 2010; Jazayeri et al., 2006). RPA (replication protein A), an eukaryotic single stranded DNA (ssDNA)-binding heterotrimeric protein composed of subunits RPA1, RPA2 and RPA3, plays crucial roles in DNA repair and replication stress to maintain genome integrity (Fanning et al., 2006). ssDNA can be recognised by RPA, which recruits the ATR/ATRIP complex and generates a platform to activate the ATR signalling cascade (Zou and Elledge, 2003). Defects in DDR affect genome instability and cell survival (Jazayeri et al., 2006).

Genome instability arising from DDR defects in early embryos or transmitted from germ cells might result in human diseases, including cancers and abnormal reproductive outcomes (O'Driscoll and Jeggo, 2006). Because of a lack of efficient DNA damage checkpoints, the mouse oocyte is comparatively tolerant of the accumulation of DNA lesions (Marangos and Carroll, 2012). Genetic lesions induced by DNA-damaging agents in mouse sperm are repaired in fertilised eggs (Generoso et al., 1979). DNA demethylation is accompanied by the appearance of the DNA damage signal in mouse zygotes (Hajkova et al., 2010; Wossidlo et al., 2010). Thus, DDR might contribute to mouse early embryonic development by cooperating with important events within the programmed implantation window (Kojima et al., 2014; Zeng and Schultz, 2005).

DDR depends on maternal mRNAs and proteins in newly fertilised zygotes, in which transcription activity is essentially lacking (Brandriff and Pedersen, 1981; Li et al., 2010). DDR can be detected almost immediately after fertilisation and as early as the G1 phase (Toyoshima et al., 2005). Preventing the RPA complex from binding to DNA by mutating RPA1 results in embryonic lethality at the blastocyst stage (Wang et al., 2005). Genetic mutations in *Atr* and other important DNA damage repair genes such as *Chk1* (checkpoint kinase 1, also known as *Chek1* – Mouse Genome Informatics) and *Rad50* (RAD50 homologue) lead to early embryonic lethality during the perimplantation stage (Brown and Baltimore, 2000; Liu et al., 2000; Luo et al., 1999; Takai et al., 2000). The embryonic lethality of these mutants impedes investigation into the maternal function of DDR genes. Until now, only maternal PMS2 (postmeiotic segregation increased 2), a mammalian homologue of a bacterial DNA mismatch repair protein, is reported to play a role in DDR in mouse development (Larson et al., 2004). Embryos lacking maternal UBE2A (ubiquitin-conjugating enzyme E2A), a homologue of the ubiquitin-conjugating enzyme RAD6 involved in DNA repair in yeast, arrest development at the two-cell stage. However, whether UBE2A is involved in DNA repair in mouse early embryos has not been analysed (Roest et al., 2004). Currently, elucidation of how maternal DDR functions in early mouse development remains elusive.

Bcas2 (breast carcinoma amplified sequence 2) was originally identified by gene amplification in human breast cancer cells (Nagasaki et al., 1999). Subsequently, BCAS2 has been identified

[1]State Key Laboratory of Stem Cell and Reproductive Biology, Institute of Zoology, Chinese Academy of Sciences, Beijing 100101, China. [2]University of Chinese Academy of Sciences, Beijing 100049, China. [3]National Institute of Biological Sciences, Beijing 102206, China. [4]Life Sciences Institute and Innovation Center for Cell Signaling Network, Zhejiang University, Hangzhou, Zhenjiang 310058, China. [5]College of Biological Science and Engineering, Beijing University of Agriculture, Beijing 102206, China. [6]School of Life Sciences and Technology, Tongji University, Shanghai 200092, China.
*These authors contributed equally to this work

[‡]Authors for correspondence (gaoshaorong@tongji.edu.cn; lil@ioz.ac.cn)

Received 14 August 2015; Accepted 24 September 2015

Development (2015) 142, 3943-3953 doi:10.1242/dev.129841

as a core component of PRP19, a pre-mRNA splicing complex (Ajuh et al., 2000). BCAS2 downregulates p53 (transformation related protein 53, also known as TRP53 – Mouse Genome Informatics or TP53 – HUGO Gene Nomenclature Committee) in the presence of DNA damage in MCF-7 cells (Kuo et al., 2009). BCAS2 interacts directly with RPA in DNA damage repair in HEK293T and HeLa cells (Maréchal et al., 2014; Wan and Huang, 2014). However, the physiological roles of BCAS2 in mammals are unknown. In the current study, we find that BCAS2 responds to endogenous and exogenous DNA damage in mouse zygotes and demonstrate its vital role in the maintenance of genomic integrity during mouse preimplantation development, potentially through interaction with RPA.

RESULTS

BCAS2 responds to DNA damage in mouse zygotes

Bcas2 mRNA and protein profiles were examined by quantitative RT-PCR (qRT-PCR) and western blot in mouse oocytes and preimplantation embryos. *Bcas2* transcript and protein levels were comparatively high in germinal vesicle (GV) oocytes, decreased in metaphase II (MII) oocytes, further reduced after fertilisation until the two-cell stage, elevated in morulas, and increased in blastocyst stage embryos (Fig. 1A,B). BCAS2 protein localisation in mouse oocytes and preimplantation embryos was further investigated by immunofluorescent staining. BCAS2 localised to nuclei in oocytes and at all stages of mouse preimplantation embryos except for MII oocytes (Fig. 1C).

BCAS2 is involved in pre-mRNA splicing and DDR as described above. However, splicing is not inefficient in the mouse zygote (Abe et al., 2015). To determine whether BCAS2 was involved in DNA repair in mouse zygotes, the correlation between BCAS2 and γH2AX, a marker of DNA damage, was assessed in zygotes of relevant pronuclear stages (PN) by staining. Mouse zygotes at various PN stages were obtained 23 h (PN2), 25 h (PN3), 28 h (PN4), and 30 h (PN5) post-hCG at embryonic day (E)0.5 and stained with traditional staining conditions (PT conditions, PFA–Triton). BCAS2 appeared in PN2-5 stage embryos, and BCAS2 staining intensity was stronger in paternal pronuclei than in maternal pronuclei in PN3 to PN5 zygotes, which correlated with γH2AX staining (Fig. 2A). Furthermore, under TP (Triton–PFA) conditions, BCAS2 foci colocalised with γH2AX in the pronuclei of PN3 to PN5 zygotes (Fig. 2B), suggesting its potential role in DDR in mouse zygotes.

Because γH2AX and BCAS2 foci colocalised more frequently in the paternal pronuclei of mouse zygotes, we induced DNA double strand breaks (DSBs) in MII oocytes to examine whether BCAS2 responds to exogenous DNA damage in zygotes (Fig. 2C). MII oocytes were treated with ultraviolet light (UV), a common treatment to induce DSBs, and fertilised with normal sperm (Bradley and Taylor, 1981; Masui and Pedersen, 1975). Few mouse zygotes developed into two-cell embryos when MII oocytes were irradiated with a high dosage of UV irradiation (0.42 J/cm^2) (data not shown). After lowering the UV dosage (0.21 J/cm^2), the majority of zygotes underwent the pronuclear stage and developed into two-cell embryos with a severe delay (data not shown). UV-induced DSBs were evidenced by increased staining of γH2AX, Ser15-phosphorylated p53 and CHK1 in maternal pronuclei (Fig. S1). Having determined the proper UV dosage (0.21 J/cm^2), irradiated MII oocytes were fertilised with normal sperm. Subsequently, zygotes were cultured for 10 h and stained with BCAS2 and γH2AX antibodies. Compared with the controls, BCAS2 and γH2AX foci accumulated in the maternal pronuclei of zygotes (Fig. 2D). These data show that BCAS2 responds to UV-induced DSBs by localizing to DNA damage sites, supporting the potential role of BCAS2 in DNA repair in mouse zygotes.

BCAS2 is crucial for female mouse fertility

To investigate whether BCAS2 functions in DNA repair in early embryos, a mouse line with a conditionally targeted *Bcas2* allele was established by flanking its exons 3 and 4 with LoxP

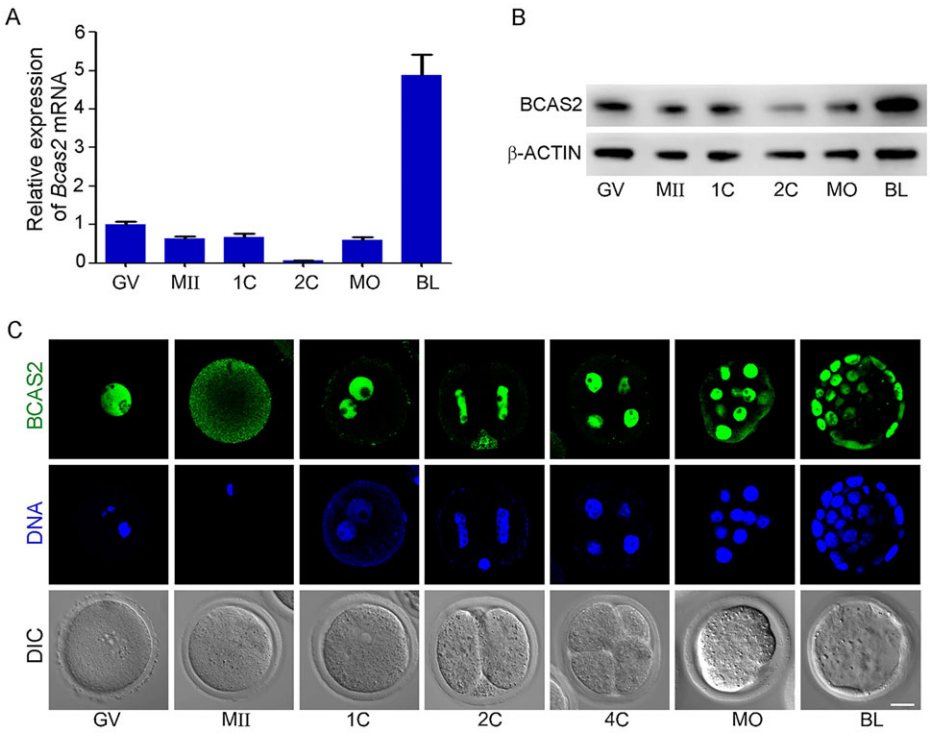

Fig. 1. The dynamics of BCAS2 expression in mouse oocytes and early embryos. (A) Quantitative RT-PCR analysis of germinal vesicle (GV) oocytes, metaphase II (MII) oocytes, zygotes (1C), two-cell (2C), morula (MO), and blastocyst (BL) stage embryos. RNA expression in GV oocytes was set as one. Data represented as mean±s.e.m. from three independent experiments. (B) Expression of BCAS2 in oocytes and preimplantation embryos (*n*=50) were analysed by western blotting. (C) Localisation of BCAS2 at various stages in oocytes and early embryos was investigated by immunostaining with anti-BCAS2 antibody and Hoechst nuclear stain. Scale bar: 20 µm.

Development (2015) 142, 3943-3953 doi:10.1242/dev.129841

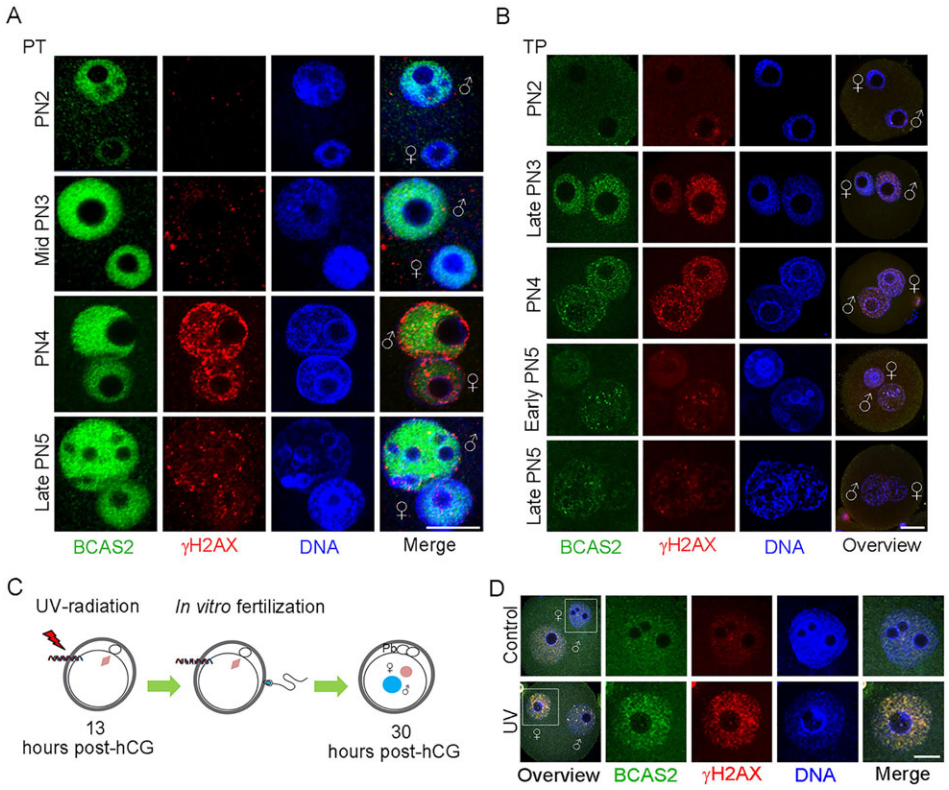

Fig. 2. BCAS2 responses to endogenous and exogenous DNA damage in mouse zygotes. (A,B) Zygotes were obtained from the oviduct at 23, 25, 28 and 30 h post-hCG, stained with antibodies against BCAS2 and γH2AX using PT (A) or TP (B) conditions, and imaged to investigate the relative localisation of BCAS2 to endogenous DNA damage. (C) Illustration of UV-induced DNA damage in MII oocytes. (D) To investigate the response of BCAS2 to exogenous DNA damage, MII oocytes were irradiated by UV for 5 min and subjected to *in vitro* fertilisation. Zygotes were cultured for 10 h and fixed after pre-extraction (at least three independent IVFs). ♂, male pronuclei; ♀, female pronuclei. Scale bars: 20 µm (A,B); 10 µm (D).

sites (Fig. S2). $Bcas2^{+/fl\text{-}Neo}$ (fl, flox) mice were viable and fertile. However, no $Bcas2^{fl\text{-}Neo/fl\text{-}Neo}$ mice resulted from mating $Bcas2^{+/fl\text{-}Neo}$ males and females (data not shown), suggesting that the inserted Neo cassette might disrupt BCAS2 function and result in embryonic lethality. After deleting the Neo cassette from $Bcas2^{+/fl\text{-}Neo}$ mice by mating with *Rosa26-Flp* mice (Rodriguez et al., 2000), $Bcas2^{fl/fl}$ mice were obtained.

To investigate BCAS2 function in mouse oocytes, $Bcas2^{fl/fl}$ females were mated with *Zp3-Cre* males (Lewandoski et al., 1997). $Bcas2^{fl/fl}$*;Zp3-Cre* mice were obtained by mating $Bcas2^{fl/+}$*;Zp3-Cre* mice and genotyped with PCR (Fig. S2, Fig. S3A). $Bcas2^{fl/fl}$*;Zp3-Cre* females and males grew to adults and appeared grossly normal. However, $Bcas2^{fl/fl}$*;Zp3-Cre* females did not deliver offspring after mating with normal males over three months (Fig. 3A). Unless otherwise stated, $Bcas2^{fl/+}$*;Zp3-Cre* and $Bcas2^{fl/fl}$*;Zp3-Cre* oocytes and embryos are hereafter designated control and $Bcas2^{mNull}$, respectively. Compared with controls, the *Bcas2* mRNA level was reduced by 95% (Fig. 3B), and BCAS2 protein was almost absent in $Bcas2^{mNull}$ oocytes (Fig. 3C,D). These data show that BCAS2 plays important roles in female mouse fertility.

Maternal BCAS2 is required for mouse preimplantation development

To examine the potential role of BCAS2 in oogenesis, ovaries from control ($Bcas2^{fl/+}$*;Zp3-Cre*) and $Bcas2^{fl/fl}$*;Zp3-Cre* females were fixed and sectioned for histological analysis. Ovaries from $Bcas2^{fl/fl}$*;Zp3-Cre* females included all stage follicles and corpora lutea and were indistinguishable from controls (Fig. S3B). In addition, superovulation resulted in similar MII oocyte morphology and number between the control and $Bcas2^{mNull}$ groups (Fig. S3C,D). These data suggest that BCAS2 might be not essential for oocyte maturation and ovulation in $Bcas2^{fl/fl}$*;Zp3-Cre* females.

Next, mouse embryos were recovered at E0.5, E1.5, E2.5 and E3.5 after mating $Bcas2^{fl/+}$*;Zp3-Cre* and $Bcas2^{fl/fl}$*;Zp3-Cre* females with wild-type males. Compared with controls, $Bcas2^{mNull}$ zygotes and two-cell embryos were almost normal in morphology and number (E0.5 and E1.5, Fig. 3E,F). However, the majority of $Bcas2^{mNull}$ embryos arrested at the two- to four-cell stages at E2.5 and E3.5, when most control embryos were at the morula and blastocyst stages, respectively (E2.5 and E3.5, Fig. 3E,F).

To further examine the defects, embryos were recovered at E0.5 and E1.5 and cultured *in vitro* to develop into the next cleavage stage. The rate of $Bcas2^{mNull}$ zygotes progressing into the two-cell stage was similar to controls (Fig. 3G), but the rate of two-cell embryos progressing into the four-cell stage was much lower than in controls (Fig. 3H), suggesting a delayed transition from the two- to the four-cell stage in $Bcas2^{mNull}$ embryos. These results indicate that maternal BCAS2 is required for mouse preimplantation development.

DNA damage repair is defective in $Bcas2^{mNull}$ early embryos

The observed accumulation of BCAS2 and γH2AX foci in the maternal pronuclei of zygotes exposed to exogenous DNA damage (Fig. 2D) prompted us to investigate the role of BCAS2 in DNA repair. To address this, two-cell embryos were recovered at 33 h (G0), 37 h (mid/late S-phase) and 48 h post-hCG (late G2 phase) at E1.5 (Artus and Cohen-Tannoudji, 2008) and stained with anti-γH2AX antibody. The γH2AX staining was mostly diffuse in the nuclei of control (n=10) and $Bcas2^{mNull}$ two-cell (n=12) embryos recovered at 33 h post-hCG (Fig. 4A). At 37 h post-hCG, γH2AX foci increased in both control and $Bcas2^{mNull}$ two-cell embryos (Fig. 4A,B). The number of γH2AX foci was similar in control (n=13) and $Bcas2^{mNull}$ embryos (n=34). However, large γH2AX foci were frequently observed in $Bcas2^{mNull}$ embryos (Fig. 4A,B).

Development (2015) 142, 3943-3953 doi:10.1242/dev.129841

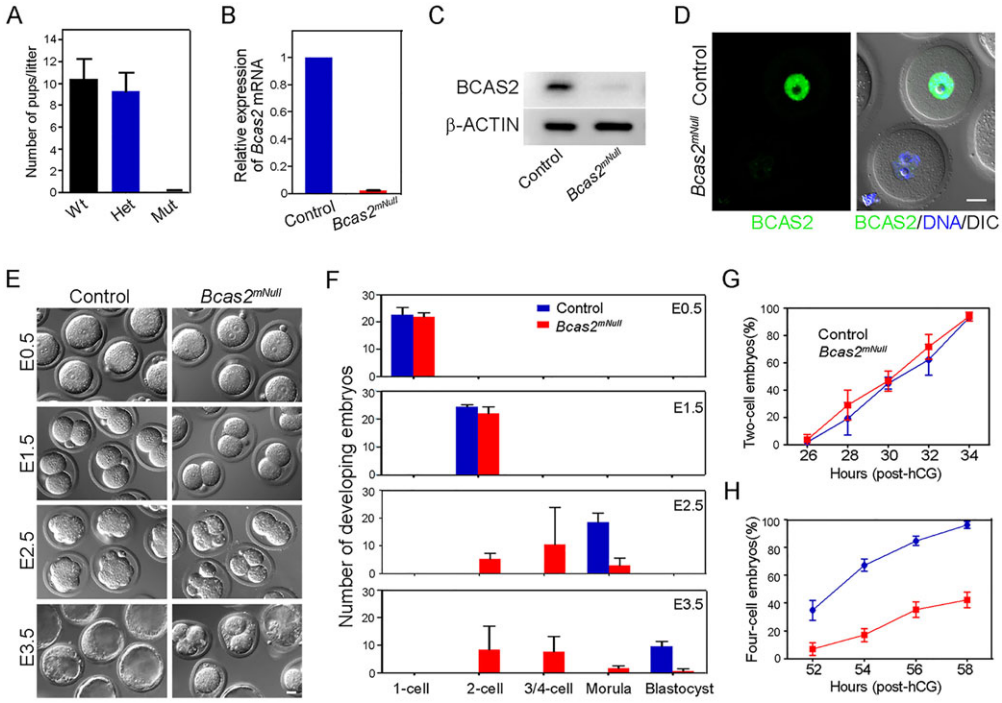

Fig. 3. Maternal depletion of BCAS2 leads to developmental arrest. (A) Wild type (Wt), *Bcas2*$^{fl/-}$ (Het) and *Bcas2*$^{fl/fl}$*;Zp3-Cre* (Mut) females were mated with normal fertile males over three months. The average number of pups per litter from the females (n=9) was analysed. The error bars represent the standard deviation (s.d.). (B) Total RNA samples prepared with n=50 control and *Bcas2*^{mNull} oocytes and subjected to real-time RT-PCR show no expression of *Bcas2* mRNA in *Bcas2*^{mNull} oocytes. Error bars represent s.e.m. (C,D) Western blotting (C) and immunostaining of oocytes fixed without pre-extraction (D) performed with control and *Bcas2*^{mNull} oocytes with antibodies against BCAS2 showed highly reduced expression of BCAS2 in *Bcas2*^{mNull} oocytes. (E,F) *Bcas2*$^{fl/+}$*;Zp3-Cre* and *Bcas2*$^{fl/f}$*;Zp3-Cre* females were superovulated and mated with normal fertile males. Control and *Bcas2*^{mNull} embryos were flushed from the oviducts of fertilised females at E0.5, E1.5, E2.5 and E3.5. The developmental stages of embryos were affirmed according to blastomere number. Average numbers of embryos are shown at different stages derived from five *Bcas2*$^{fl/+}$*;Zp3-Cre* and *Bcas2*$^{fl/fl}$*;Zp3-Cre* females. (G) Zygotes were flushed from the oviducts at 26 h post-hCG and cultured in KSOM to develop into two-cell embryos. Developmental rates were determined from five females. (H) Two-cell embryos were flushed from oviducts at 52 h post-hCG and cultured in KSOM into the four-cell stage. Developmental rates were calculated without the amount of arrested two-cell embryos. Error bars represent s.e.m. Scale bars: 20 µm.

At 48 h post-hCG, γH2AX foci were dramatically reduced in control embryos (n=65) but remained at significantly higher levels in *Bcas2*^{mNull} embryos (n=46) (Fig. 4A,B).

To investigate whether increased γH2AX expression in *Bcas2*^{mNull} two-cell embryos was caused by developmental delay, we stained *Bcas2*^{mNull} embryos (48 post-hCG) with phosphorylated

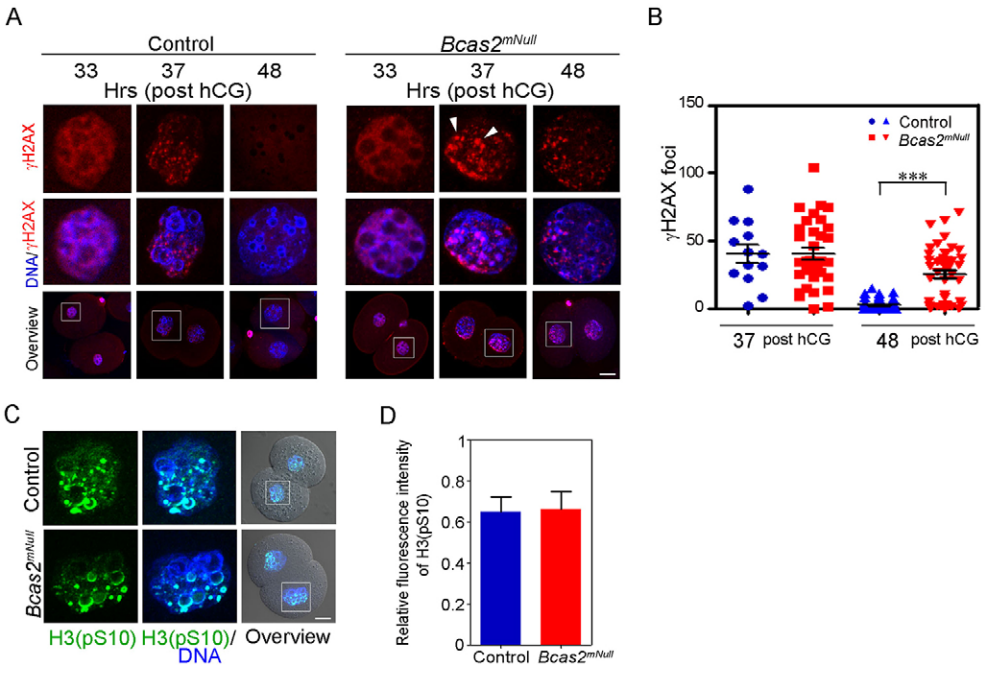

Fig. 4. DNA damage accumulates in *Bcas2*^{mNull} two-cell embryos. (A) Representative images of control and *Bcas2*^{mNull} two-cell embryos obtained at 33, 37 and 48 h post-hCG and stained with γH2AX and BCAS2 antibodies. Large γH2AX foci were observed in *Bcas2*^{mNull} embryos (white arrowheads). (B) Two-cell embryos obtained at 37 and 48 h post-hCG were stained as in A. γH2AX foci in embryos were quantified with ImageJ software. (C) Representative images of two-cell embryos (48 h post-hCG) stained with a marker of late G2/M-phase, phosphorylated H3S10 [H3 (pS10)], using TP conditions. (D) Quantification of phosphorylated H3S10 intensity normalised against DNA staining by Hoechst and analysed with ImageJ. The error bars represent the s.e.m. from three independent experiments. ***P<0.001. Scale bars: 20 µm.

Development (2015) 142, 3943-3953 doi:10.1242/dev.129841

H3S10, a marker of late G2/M-phase (Goto et al., 1999). When normalised to DNA staining by Hoechst, both controls (n=30), and *Bcas2*^{mNull} embryos (n=30) shared a similar intensity of phosphorylated H3S10 signal (Fig. 4C,D), suggesting that the majority of *Bcas2*^{mNull} two-cell embryos entered G2-phase at 48 post-hCG with damaged DNA in the same way as control two-cell embryos. This would indicate that increased γH2AX is not a result of developmental delays in *Bcas2*^{mNull} two-cell embryos, and together, these data suggest the BCAS2 plays an important role in DNA repair in mouse early embryos.

DNA damage activates checkpoints in *Bcas2*^{mNull} two-cell embryos

The damaged DNA in *Bcas2*^{mNull} two-cell embryos might activate p53 to delay cell cycle progression (Shiloh, 2001). To test this, *Bcas2*^{mNull} embryos recovered at 48 h post-hCG were stained with anti-phosphorylated p53 antibody. Compared with control, phosphorylated p53 increased in *Bcas2*^{mNull} two-cell embryos (Fig. 5A). Western blotting further confirmed the increased level of γH2AX and phosphorylated p53 (Fig. 5B). In response to DNA damage, the activation of p53 usually triggers the expression of *p21* (cyclin-dependent kinase inhibitor 1A, also known as *Cdkn1a* – Mouse Genome Informatics) and *Gadd45a* (growth arrest and DNA-damage-inducible 45 alpha) to arrest the cell cycle (Brugarolas et al., 1995; Siafakas and Richardson, 2009). Thus, these p53 targets in *Bcas2*^{mNull} embryos were examined by qRT-PCR. Compared with controls, the expression of *Gadd45a* was not significantly changed. However, *p21* mRNA significantly increased in *Bcas2*^{mNull} two-cell embryos (Fig. 5C).

Subsequently, we tested whether p53 inhibition could alleviate the two-cell arrest of *Bcas2*^{mNull} embryos. To this end, *in vitro* fertilised *Bcas2*^{mNull} zygotes were treated with Pifithrin-α, a specific inhibitor of p53-dependent transcriptional activation, and cultured for 43 h. Compared with 0.1% DMSO treatment (control), Pifithrin-α significantly decreased the percentage of arrested *Bcas2*^{mNull} two-cell embryos (Fig. 5D,E). Furthermore, Pifithrin-α significantly decreased the expression of *p21* and *Gadd45a* in *Bcas2*^{mNull} two-cell embryos (Fig. 5F). These results suggest that the delayed or arrested development of *Bcas2*^{mNull} two-cell embryos is partially as a result of damaged DNA and the subsequent activation of p53.

Considering the relatively limited ability of Pifithrin-α to alleviate the developmental arrest of *Bcas2*^{mNull} two-cell

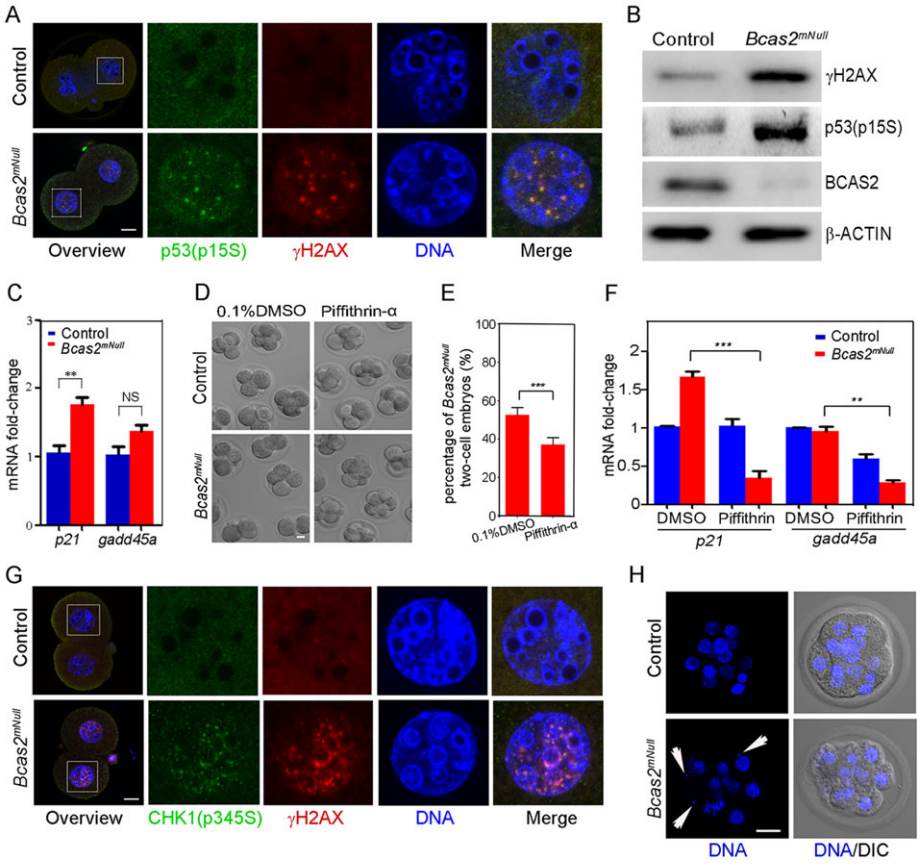

Fig. 5. Checkpoints are activated in *Bcas2*^{mNull} two-cell embryos. (A) Control and *Bcas2*^{mNull} two-cell embryos were harvested at 48 h post-hCG and stained with anti-p53 (p15S) and anti-γH2AX antibodies. (B) Control and *Bcas2*^{mNull} two-cell embryos were recovered at 48 h post-hCG and subjected to western blotting. (C) Levels of *p21* and *Gadd45a* mRNA were analysed in two-embryos obtained at 48 h post-hCG by qRT-PCR. (D) *Bcas2*^{mNull} zygotes (n=743) from IVF were cultured in KSOM containing either 0.1% DMSO or 100 µM Pifithrin-α for 43 h and imaged. Pifithrin-α treatment did not alter the development of normal embryos compared with DMSO treatment. (E) *Bcas2*^{mNull} two-cell embryos from D were counted in individual culture drops. The percentage of two-cell embryos was calculated by dividing the number of all embryos in an individual drop. Binary logistic repression was used to analyse statistical significance, and the number of two-cell oocytes was found to be significantly lower on treatment with Pifithrin-α (***P<0.001). (F) Levels of *p21* and *Gadd45a* mRNA were measured in *Bcas2*^{mNull} two-cell embryos obtained at 48 h post-hCG from D using qRT-PCR with specific primers (Table S4). ***P<0.005, **P<0.01. (G) Control and *Bcas2*^{mNull} two-cell embryos were harvested at 48 h post-hCG and stained with anti-phosphor-CHK1 (S345) and anti-γH2AX antibodies. (H) Control and *Bcas2*^{mNull} embryos were obtained at E2.5 and stained with Hoechst to detect micronuclei (arrowheads) caused by unrepaired DNA damage. Scale bars: 20 µm. Data in C,E,F are represented as the mean±s.e.m. calculated from three independent experiments.

Development (2015) 142, 3943-3953 doi:10.1242/dev.129841

embryos, other pathways might also be involved in the arrest of *Bcas2*^{mNull} embryos. DNA damage activates the WEE1/CDC25 pathway that is regulated by CHK1, which arrests the cell cycle at interphase by stimulating the CDC2-cyclin B complex (O'Connell et al., 1997; Sanchez et al., 1997). In normal mouse two-cell embryos, CHK1 was phosphorylated at S-phase and then decreased at the late G2 stage during cell cycle progression (Fig. S4). To examine whether CHK1/CDC25 was activated in *Bcas2*^{mNull} two-cell embryos, control and *Bcas2*^{mNull} two-cell embryos recovered at 48 h post-hCG were immunostained for pCHK1. pCHK1 staining was almost absent in controls (n=30) but was observed in 48% of *Bcas2*^{mNull} two-cell embryos (n=25) (Fig. 5G).

In addition to DNA damage checkpoints, malfunction of zygotic genome activation (ZGA) also causes two-cell stage arrest (Bultman et al., 2006; Posfai et al., 2012; Wu et al., 2003). When the expression of ZGA genes (Zeng et al., 2004; Zeng and Schultz, 2005) was examined by quantitative RT-PCR, the mRNA levels of ZGA genes such as *Tdpoz1*, *Tdpoz3*, *Tdpoz4* increased. However, the expression of other ZGA genes (*Gm13043* and *Ccnjl*) decreased (Fig. S7) or remained unaffected (*Zscan4a*, *H2-Q6* and *Prss8*, data not shown), suggesting that ZGA is partially affected in *Bcas2*^{mNull} two-cell embryos and might also contribute to delayed or arrested development.

Unrepaired DNA damage endangers cells with risks of genome instability, including abnormal micronuclei (Takai et al., 2000). To examine if micronuclei were present in *Bcas2*^{mNull} embryos, DNA was stained with Hoechst. Micronuclei were not observed in control embryos. However, 40% (n=40) of *Bcas2*^{mNull} embryos surviving beyond the two-cell stage had micronuclei (Fig. 5H). These data suggest that BCAS2 disruption leads to the accumulation of damaged DNA and activates checkpoints in *Bcas2*^{mNull} two-cell embryos, which might arrest mouse development at early embryonic stages.

BCAS2 functions in DNA repair in mouse zygotes

To examine DNA repair defects in mouse zygotes, embryos were recovered at 23, 25, 28 and 30 h post-hCG (PN2, PN3, PN4, PN5, respectively) and stained with anti-γH2AX antibody. In control zygotes, γH2AX foci initially appeared at PN2, dramatically increased at PN3 and PN4, and almost disappeared at late PN5 (Fig. 6A, left panel). The number of γH2AX foci did not significantly increase during PN2 to PN4 (data not shown). However, enlarged

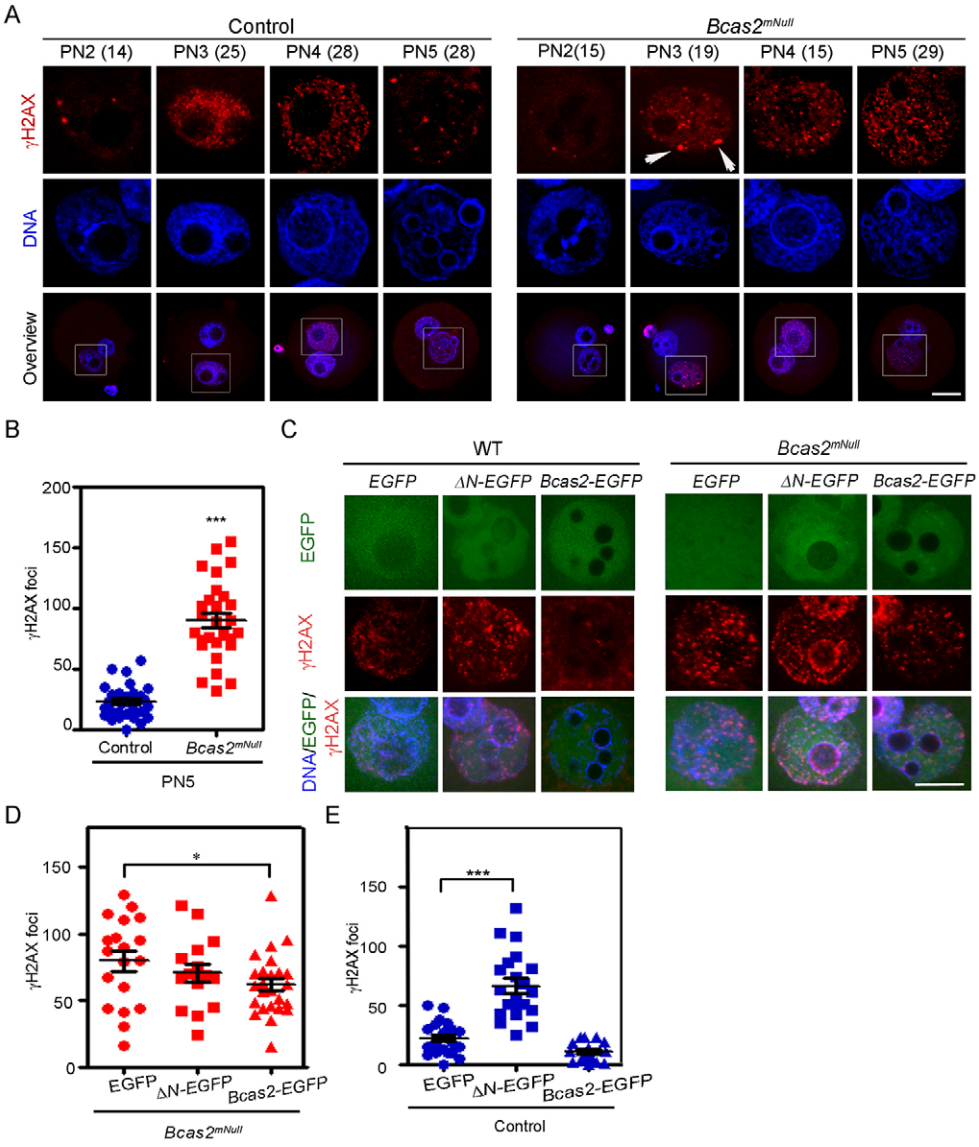

Fig. 6. BCAS2 is required for DNA repair in mouse zygote. (A) Control and *Bcas2*^{mNull} zygotes were obtained at 23, 25, 28 and 30 h post-hCG and stained with anti-γH2AX antibody. White arrowheads indicates large γH2AX foci in *Bcas2*^{mNull} zygotes. The number of analysed zygotes at indicated stages is given in parentheses. (B) Quantification of γH2AX foci in both pronuclei of individual zygotes obtained at 30 h post-hCG. (C) Wild-type (WT) and *Bcas2*^{mNull} zygotes were obtained at 23 h post-hCG and microinjected with *EGFP*, *ΔN-EGFP* or *EGFP*-tagged *Bcas2* mRNA. Microinjected zygotes were cultured for 7-8 h and stained with anti-γH2AX antibody. (D,E) Quantification of γH2AX foci in individual zygotes from C. Error bars represent s.e.m. from three independent experiments. *P<0.05, ***P<0.001. Scale bars: 20 µm.

Development (2015) 142, 3943-3953 doi:10.1242/dev.129841

γH2AX foci were observed in *Bcas2*^{mNull} PN3 zygotes (Fig. 6A, right panel). Strikingly, compared with the control at late PN5 in which γH2AX foci almost disappeared, γH2AX foci persisted in *Bcas2*^{mNull} zygotes (Fig. 6A,B). DNA fragmentation was further confirmed in *Bcas2*^{mNull} PN5 zygotes by TUNEL assay (Fig. S6).

Next, we tested whether re-expression of BCAS2 could repair the damaged DNA in *Bcas2*^{mNull} zygotes. *Bcas2*^{mNull} zygotes were recovered at 23 h post-hCG and microinjected with EGFP-tagged *Bcas2* mRNA or control (EGFP). The injected zygotes were cultured for 7 h until the PN5 stage and stained with anti-γH2AX antibody. γH2AX foci were partially reduced in the *Bcas2*^{mNull} zygotes injected with *EGFP-Bcas2* mRNA but not in the *Bcas2*^{mNull} zygotes injected with *EGFP* (Fig. 6C,D). These results further support a BCAS2 function in DNA repair in mouse zygotes.

BCAS2-mediated DNA repair facilitates replication in mouse zygotes

DNA replication mainly initiates at PN3 in mouse zygotes (Ferreira and Carmo-Fonseca, 1997). The observation of enlarged γH2AX foci at PN3 in *Bcas2*^{mNull} zygotes (Fig. 6A, arrows) led us to suspect that the defects in DNA repair might disrupt DNA replication in *Bcas2*^{mNull} zygotes. To test this, control and *Bcas2*^{mNull} zygotes were recovered at 25, 28 and 30 h post-hCG, and pronuclear formation was examined. Most control and *Bcas2*^{mNull} zygotes developed into PN3 (25 h), PN4 (28 h) and PN5 (30 h). Then, these embryos were cultured with EdU for 30 min prior to fixation and stained with EdU. In controls, the EdU signal was almost equally diffused in both parental pronuclei at PN3 and in the peripheral regions of both pronuclei at PN4 (Fig. 7A, left panel), consistent with a previous report (Wossidlo et al., 2010). However, the EdU signal was either weak or absent in PN3 and PN4 *Bcas2*^{mNull} zygotes (Fig. 7A, right panel; Fig. 7B). PN3 and PN4 zygotes labelled with EdU were further quantified. In controls, 87% (n=32) of PN3 and 83% (n=45) of PN4 zygotes were labelled with EdU. However, only 51% (n=26) of PN3 and 38% (n=31) of PN4 *Bcas2*^{mNull} zygotes were labelled with EdU (Fig. 7B). At the late PN5 stage, control zygotes (n=15) were not labelled with EdU. However, 64% (9/14) of *Bcas2*^{mNull} zygotes were still labelled with EdU (Fig. 7B). These data demonstrate that *Bcas2*^{mNull} embryos have impaired DNA replication, suggesting that unrepaired DNA breaks cause replication stress during pronuclear stages in mouse zygotes.

To further investigate the role of BCAS2-mediated DNA repair in recovering from replication stress, zygotes were treated with hydroxyurea (HU), a general DNA damaging agent that stalls or breaks replication forks. Control and *Bcas2*^{mNull} zygotes were recovered at 25 h post-hCG and exposed to HU for 3 h. After HU release, these embryos were cultured for 23 h to develop into two-cell embryos. Approximately 55% of control zygotes (n=121) developed into two-cell embryos, whereas only 22% of *Bcas2*^{mNull} zygotes (n=132) progressed to the two-cell stage (Fig. 7C). These data suggest that the capability to recover from replication stress is impaired in *Bcas2*^{mNull} zygotes.

BCAS2 functions in mouse zygotes through the RPA complex

The RPA complex, a well-known sensor in response to replication stress, is composed of RPA1, RPA2 and RPA3 (Fanning et al., 2006; Zou and Elledge, 2003). BCAS2 lacking the 139 N-terminal bases fails to interact with RPA1 (Wan and Huang, 2014), prompting us to examine whether the interaction between BCAS2 and RPA1 was required for DNA repair in mouse zygotes. Normal zygotes at PN2 were injected with *Bcas2* mRNA lacking the

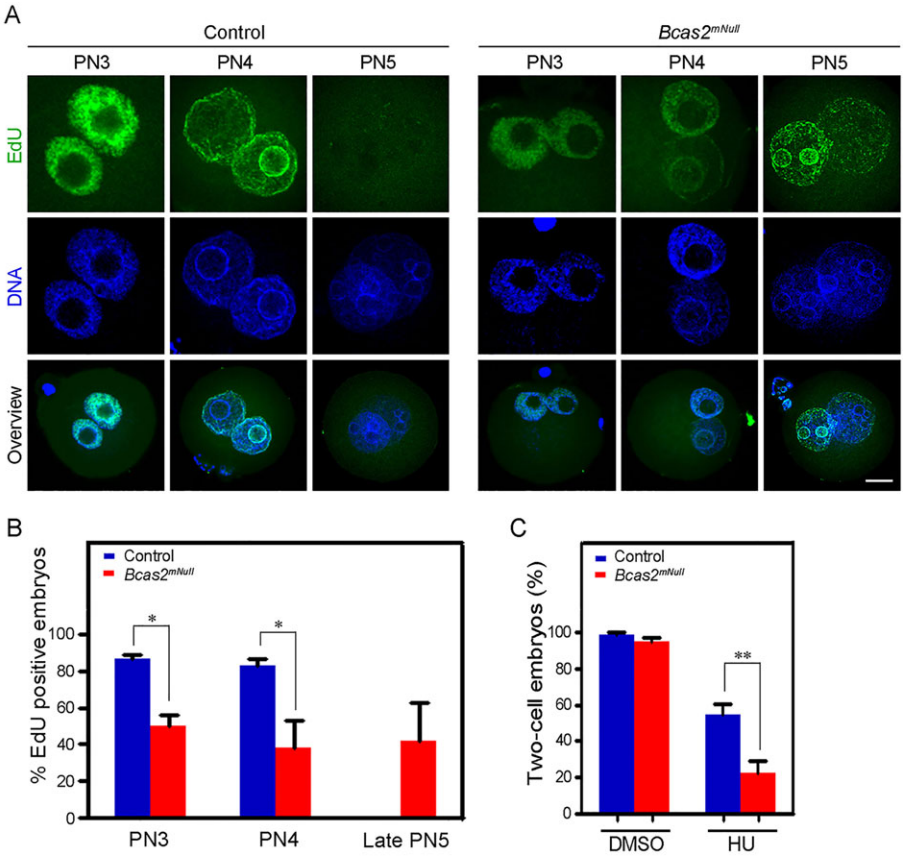

Fig. 7. BCAS2-mediated DNA repair is involved in DNA replication in mouse zygotes. (A) Control and *Bcas2*^{mNull} zygotes were obtained at 25, 28 and 30 h post-hCG, cultured with EdU for 30 min prior to fixation, stained and imaged. (B) Quantification of EdU-positive zygotes from A. (C) Control and *Bcas2*^{mNull} zygotes were exposed to HU for 3 h and cultured for 23 h until the late two-cell stage. Numbers of two-cell embryos were counted in control and HU treated groups. Error bars represent s.e.m. from three to five independent experiments. *P<0.05, **P<0.01. Scale bar: 20 µm.

Development (2015) 142, 3943-3953 doi:10.1242/dev.129841

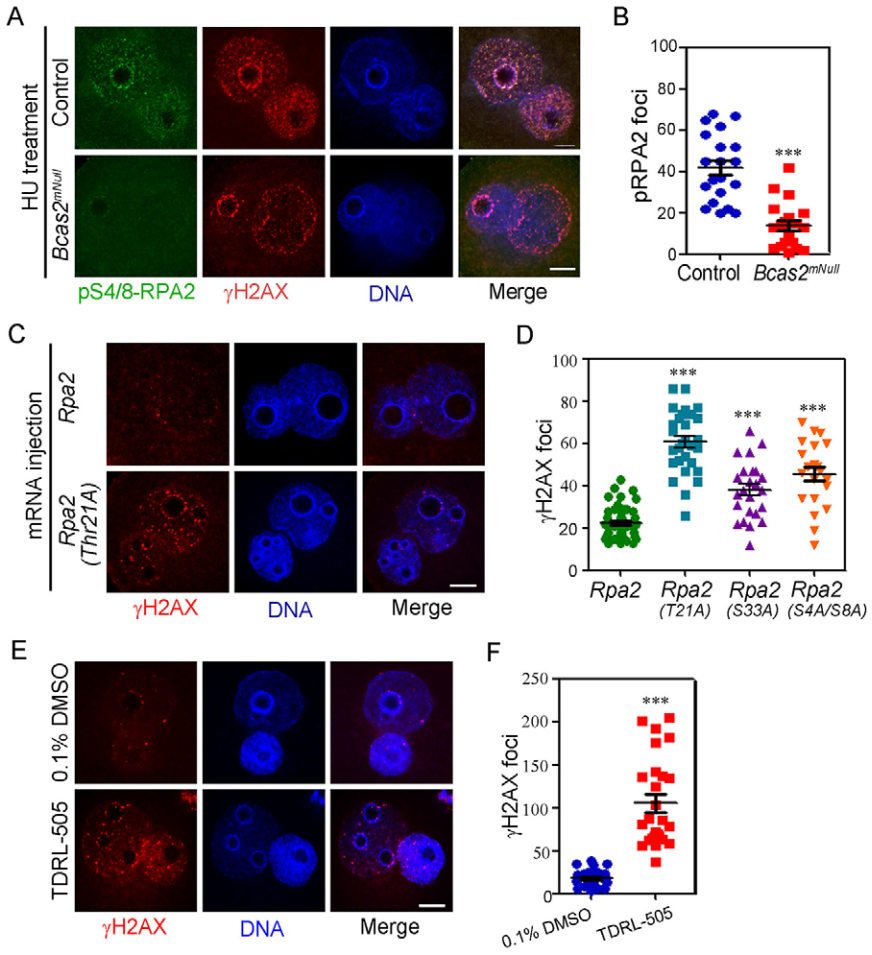

Fig. 8. BCAS2-mediated DNA repair functions through RPA. (A) Control and *Bcas2*^{mNull} zygotes were obtained at 25 h post-hCG and exposed to HU for 5 h. Zygotes were fixed and stained with anti-γH2AX antibody. (B) Quantification of phosphorylated RPA2 foci in both pronuclei of control and *Bcas2*^{mNull} zygotes from A. (C) Normal zygotes were injected with either wild-type or Thr21A mutant *Rpa2* mRNA, cultured for 7-8 h in KSOM prior to fixation and stained with anti-γH2AX antibody. (D) Quantification of γH2AX foci in both pronuclei of normal zygotes injected with either wild-type or mutant (Ser4A/8A, Thr21A and Ser33A) *Rpa2* mRNA and stained as in C. (E) Zygotes were harvested 25 h post-hCG, cultured for 5 h in KSOM containing 50 µM TDRL-505, fixed, stained with anti-γH2AX antibody and imaged. (F) Quantification of γH2AX foci in both pronuclei in zygotes from E. Error bars represent s.e.m. from three independent experiments. ***P<0.001. Scale bars: 10 µm.

N-terminal 139 bases (referred as *ΔN-EGFP*), cultured until PN5 and stained with γH2AX. Compared with controls injected with *EGFP* mRNA or full-length *Bcas2-EGFP*, zygotes injected with *ΔN-EGFP* exhibited increased γH2AX foci, suggesting that BCAS2 lacking the interaction with RPA1 might function in DNA repair in mouse zygote as a dominant-negative mutant (Fig. 6C,E). Furthermore, γH2AX foci were not reduced by the injection of *ΔN-EGFP* in *Bcas2*^{mNull} zygotes compared with *Bcas2*^{mNull} zygotes injected with normal *Bcas2-EGFP* mRNA (Fig. 6C,D). These data suggest that the BCAS2 interaction with RPA1 is important for DNA repair in mouse zygotes.

In response to DNA damage, RPA2 is phosphorylated at Ser33, Ser4/Ser8, Ser12, and Thr21, promoting the binding of the RPA complex to DNA to activate DNA damage checkpoints (Anantha et al., 2007; Block et al., 2004; Oakley et al., 2003; Shi et al., 2010; Wang et al., 2001). Mutated Ser33A, Ser4/Ser8 and Thr21A phosphorylation sites in RPA2 lead to defective recovery from replication stress (Ashley et al., 2014; Olson et al., 2006). Decreased BCAS2 affects the phosphorylation of RPA2 Ser4/Ser8 (Wan and Huang, 2014), which is phosphorylated after Thr21 and Ser33 phosphorylation (Anantha et al., 2007; Liu et al., 2012). To further investigate whether BCAS2 is involved in DNA repair through the RPA complex, the activity of RPA2 in response to DNA damage was investigated in control and *Bcas2*^{mNull} zygotes treated with HU. The phosphorylated RPA2 formed numerous foci that colocalised with γH2AX in control zygotes (n=20) (Fig. 8A, upper panel), indicating that RPA2 is effectively activated in normal zygotes. However, few phosphorylated RPA2 foci were observed in *Bcas2*^{mNull} zygotes (n=19) (Fig. 8A, lower panel). Compared with control, phosphorylated RPA2 foci were significantly decreased in *Bcas2*^{mNull} zygotes (Fig. 8B). These data suggest a defect of RPA activity in responding to replication stress in the *Bcas2*^{mNull} zygotes.

To examine the involvement of the RPA complex in DNA repair at the first mouse cell cycle, normal zygotes were recovered at 23 h post-hCG (PN2) and either injected with *Rpa2* mutant (S4A/S8A, Thr21A or S33A) mRNA or treated with TDRL-505, an inhibitor blocking the formation of RPA-ssDNA (Anciano Granadillo et al., 2010; Shuck and Turchi, 2010). After culturing for 7-8 h, the embryos were stained for γH2AX. Zygotes injected with normal *Rpa2* mRNA (control) had few γH2AX foci (n=51). However, embryos injected with mutant Ser4A/Ser8A (n=22), Thr21A (n=28) or Ser33A (n=23) mRNA had increased γH2AX foci in both parental pronuclei (Fig. 8C,D). In addition, TDRL-505 treatment dramatically increased γH2AX foci in PN5 zygotes (Fig. 8E,F). TDRL-505 treatment also delayed zygote development into two-cell embryos, accompanied by accumulated γH2AX foci (Fig. S7A-C). These data suggest that the RPA complex plays important roles in DNA repair in mouse zygotes.

Together, our data suggest that BCAS2 protects mouse zygotes from replication stress and DNA damage by influencing RPA function during the first cell cycle in mouse development.

DISCUSSION

BCAS2 plays important roles in alternative splicing and DNA repair in cells. Knockdown of BCAS2 by siRNA in HEK293T and HeLa

Development (2015) 142, 3943-3953 doi:10.1242/dev.129841

cells results in no obvious defects in DNA repair, but cells are defective in responses to campotothecin (CPT)-induced DNA lesions (Wan and Huang, 2014). In the present study, we demonstrated that BCAS2 responds to both exogenous and endogenous DNA lesions in mouse zygotes. Oocyte-specific ablation of BCAS2 results in the developmental arrest of cleavage-stage embryos accompanied by accumulated DNA damage and defects in DNA replication. Thus, our results suggest that BCAS2-mediated DNA repair is important to maintain the genome integrity of mouse early embryos. Persistent DNA damage in *Bcas2*^{mNull} zygotes and two-cell embryos but not in BCAS2 knockdown cells suggests that early mouse embryos might be more sensitive to damaged DNA than normal cells.

We previously showed that BCAS2 responds to CPT-induced DNA damage by interacting with RPA (Wan and Huang, 2014). Consistently, BCAS2 mutants unable to bind RPA1 failed to repair damaged DNA in mouse zygotes. Furthermore, phosphorylated RPA2 did not form foci in response to replication stress in *Bcas2*^{mNull} zygotes. In addition, disruption of the activity of the RPA complex resulted in accumulated DNA damage in mouse zygotes. Our data suggest that the maternal BCAS2 pathway potentially protects genomic integrity through the RPA complex in mouse early embryonic development.

In somatic cells, deficient DNA repair usually activates cell cycle checkpoints such as the CHK1 and p53-p21-cyclin-CDKs pathways (Arias-Lopez et al., 2006; El-Deiry et al., 1992; Espinosa et al., 2003; Jazayeri et al., 2006; Levine, 1997; Macleod et al., 1995; Miyashita and Reed, 1995). Although many mutant strains display embryonic lethality at the preimplantation stage, few mutant mouse lines exhibit embryonic lethality at early cleavage stages (Friedberg and Meira, 2006). Because of the maternal contribution of these genes, the embryonic lethal phenotypes observed in mutants deficient in DDR might underscore the importance of DDR during preimplantation development. Our finding that both the p53 and CHK1 pathways are activated in response to damaged DNA in *Bcas2*^{mNull} two-cell embryos suggests that mouse early embryos could arrest development in response to DNA damage via these pathways as early as the two-cell stage.

Bcas2^{mNull} zygotes cleaved into two-cell embryos without obvious developmental delays but arrested at the zygotic stage with increased DNA damage upon HU treatment, supporting the notion that the checkpoint is activated in a dosage dependent manner in mouse zygotes (Adiga et al., 2007; Grinfeld and Jacquet, 1987). Thus, it is possible that damaged DNA does not activate the checkpoint in *Bcas2*^{mNull} zygotes, which cleave into two-cell stage embryos. As DNA lesions accumulate and checkpoints gradually activate at the two-cell stage, *Bcas2*^{mNull} embryonic development eventually arrests at late cleavage stages. In addition, the malfunction of ZGA might also contribute to two-cell arrest in *Bcas2*^{mNull} two-cell embryos.

Because BCAS2 is involved in multiple functions in cells and as a result of the limitations of current models and analyses, we could not rule out the possibility that BCAS2 might also indirectly affect the function of RPA in DNA repair in mouse zygotes or the roles of BCAS2 during oogenesis and early development. However, established mouse embryos lacking maternal BCAS2 not only allow us to study the physiological function of BCAS2 in DNA repair during early embryonic development but might also provide useful models for elucidating the roles of BCAS2 in ZGA, DNA demethylation and other important events involved in mouse early embryogenesis.

MATERIALS AND METHODS

Mouse maintenance and gene targeting at the *Bcas2* locus

In compliance with the guidelines of the Animal Care and Use Committee of the Institute of Zoology at the Chinese Academy of Sciences, the *Bcas2*$^{loxp/loxp}$;*Zp3-Cre* mouse line was maintained on a mixed background (129/C57BL/6). To construct a conditional mouse line for targeting the *Bcas2* allele, exons 3 and 4 of *Bcas2* were flanked by LoxP sites (Fig. S2, Table S1). The recombined embryonic stem cells (ESCs) were screened by PCR with two primers (Neo-F and screen-R, Table S1), further confirmed by sequencing (data not shown), and injected into C57BL/6 blastocysts. One chimera transplanted the targeted allele through the germline, and the Neo cassette was deleted by mating *Bcas2*$^{+/fl\text{-}Neo}$ and *Rosa26-Flp* mice to produce *Bcas*$^{+/fl}$ mice (Fig. S2). Mice were genotyped using tail DNA as PCR templates with three oligo-primers (F-WT, F-KO, R, Table S1; Fig. S3A). The conditional mouse line was established by crossing *Bcas2*$^{fl/fl}$ mice with *Zp3-Cre* mice to specifically ablate BCAS2 in growing oocytes (Fig. S2). *Bcas2*^{mNull} embryos were obtained by mating *Bcas2*$^{fl/fl}$;*Zp3-Cre* females with normal males.

Fertility assessment and ovarian histology

Fertility assessment was conducted by 2:1 caging of *Bcas2*$^{fl/+}$;*Zp3-Cre* and *Bcas2*$^{fl/fl}$;*Zp3-Cre* females (n>5) with wild-type males for over three months. Successful mating was verified by the presence of a post-coital vaginal plug, after which mice were caged separately. For histology analysis, ovaries from adult females were fixed in Bouin's solution, sectioned, rehydrated, and stained with hematoxylin and 1% eosin (ZSGB-BIO).

In vitro fertilisation, culture and collection of mouse oocytes and early embryos

For *in vitro* fertilisation (IVF), MII oocytes were harvested with M2 medium from 7- to 8-week-old females after injections of PMSG and hCG (Ningbo Second Hormone Factory) and transferred into human tubular fluid (HTF) buffer. Next, 5×10^6/ml capacitation sperm were added to HTF containing MII oocytes, which were then cultured in a humidified atmosphere of 5% CO_2 for the next 6 h and then transferred to KSOM at the designated stages (Fraser and Drury, 1975).

For harvesting oocytes or embryos, females were intraperitoneally injected with PMSG and hCG. Oocytes or embryos were manipulated in M2 at the indicated time points after hCG injection: MII oocytes, 13 h; zygotes, 23-30 h; two-cell embryos, 33-48 h; morula, 71 h; blastocyst, 98 h. Germinal vesicle stage (GV) oocytes were obtained 48 h after PMSG.

Fertilisation of UV-irradiated mouse MII oocytes and chemical treatment of early embryos

MII oocytes were manipulated with M2 and transferred to HTF media covered with mineral oil. UV irradiation was performed using UV-C lamps (254 nm). After UV irradiation, MII oocytes were transferred to another HTF drop and fertilised *in vitro* with normal sperm. For UV irradiation two-cell embryo experiments, embryos were obtained at 37 h post-hCG, irradiated for 1 min, and cultured 3 h prior to fixation and staining.

For Pifithrin-α (Sigma) treatment, *Bcas2*^{mNull} zygotes from IVF were cultured for 15 h, treated with either 0.1% DMSO or 100 µM Pifithrin-α for 43 h, and imaged. At 48 h post-hCG, 25 *Bcas2*^{mNull} two-cell stage embryos that were treated with either 0.1% DMSO or 100 µM Pifithrin-α were collected for qRT-PCR. For HU and TDRL-505 treatment, control and *Bcas2*^{mNull} zygotes were recovered at 25 h post-hCG and exposed to 4 mM HU (Sigma) for 3 h or 100 µM TDRL-505 (Calbiochem) for 7-8 h. Zygotes were either fixed for immunostaining with anti-phosphorylated-RPA2 or anti-γH2AX antibody or cultured for 48 h post-hCG for assessing the percentage of embryos progressing to the two-cell stage.

Immunofluorescence staining, microscopy and image analysis

For PT (PFA–Triton) conditions, embryos were fixed in 4% PFA for 30 min at 37°C, washed three times with PBS, and permeabilised with 0.5% Triton X-100 in PBS (5 min, RT). Embryos were washed three times with PBST (PBS with 0.1% Triton X-100), blocked with 5% donkey serum (1 h, RT), incubated in primary antibodies (Table S2, overnight at 4°C), washed with

Development (2015) 142, 3943-3953 doi:10.1242/dev.129841

PBST, and incubated with secondary antibody (Table S2, 1 h at RT). The images were obtained with the LSM780 (Zeiss).

For TP (Triton–PFA) conditions, the zona pellucida of embryos were removed with acid Tyrode's solution (Sigma). Embryos were permeabilised with 0.1% Triton X-100 in PBS (PBST) for 1 min on ice and then fixed with 4% PFA (37°C, 30 min). The embryos were stained as described above.

Immunofluorescence images were analysed with ZEN lite 2011 (Zeiss). A *z*-series was performed to cover the maximal radius of individual pronuclei. For data presentation, the separated images of both pronuclei were merged.

Western blotting of oocytes and preimplantation embryos

Mouse oocytes or early embryos were washed with PBS before freezing in 10 µl RIPA containing protease inhibitor cocktail (Roche) and stored at −80°C. The samples were separated on NuPage 4-12% Bis-Tris gels with MOPS SDS running buffer and transferred to PVDF membranes (Invitrogen). The blots were pre-treated with Superblock Blocking Buffer (Thermo Fisher Scientific), incubated with primary antibodies (Table S2) overnight at 4°C, washed six times with PBST (5 min), incubated with horseradish peroxidase-conjugated secondary antibodies (Table S2, 1 h at RT), detected with SuperSignal West Dura Extended Duration Substrate (Thermo Fisher Scientific) and imaged with a LAS-3000 (FujiFilm).

EdU incorporation and TUNEL assay of mouse embryos

Embryos were recovered at E0.5 or E1.5 and cultured in KSOM containing 50 mM EdU at 37°C for 30 min prior to fixation. Detection of incorporated EdU was performed using the Cell-Light EdU Apollo 567 *In Vitro* Imaging Kit (RiboBio) according to the manufacturer's protocol. Immunofluorescent staining was performed as described above. Control and *Bcas2*^{mNull} zygotes were examined by TUNEL assay according to the manufacturer's protocol (Roche).

mRNA microinjection of mouse zygotes

Bcas2 and *Rpa2* were amplified from mouse ovary cDNA with specific primers (Table S3). *Bcas2* and *Rpa2* cDNA were inserted into modified *pEGFP-N1* and *Pcs2*$^{+}$*-myc* vectors, respectively. *Rpa2* point mutations were generated by mutating *Rpa2* (Table S3) in the *Rpa2-pcs2*$^{+}$*-myc* vector (Toyobo). Linearised plasmid was used for *in vitro* transcription with the mMESSAGE mMACHINE Kit (Ambion) and purified with an RNeasy MinElute Cleanup Kit (Qiagen). mRNA was dissolved in nuclease-free water at 100 ng/µl. Mouse zygotes before the PN3 stage were microinjected with 5-10 pl of mRNA and cultured until the next processes.

Quantitative real-time RT-PCR

The mRNA was isolated from oocytes or embryos using the Dynabeads mRNA Direct Micro Kit (Ambion). Reverse transcription of RNA was performed using PrimeScript RT Reagent Kit (Takara). Quantitative PCR was performed using EvaGreen qPCR MasterMix (Applied Biological Materials) with specific primers (Table S4). Measurements were performed with three independent biological replicates.

Analysis of γH2AX foci in zygotes and two-cell embryos

Mouse zygotes and two-cell embryos from control and *Bcas2*^{mNull} females were stained as described above. *Z*-series images were obtained to cover the maximal radius of individual pronuclei (nuclei) and were merged for each embryo by ZEN lite 2011 (Zeiss). Each picture was processed with Enhanced Contrast by saturated pixels 0.4% using ImageJ software. The foci in each picture were counted with Find Maxima by altering Noise Tolerance. The data were presented as the means±s.e.m.

Statistical analyses

Quantitative analyses were carried out with GraphPad Prism software with at least 3-5 independent biological samples and expressed as the means±s.e.m. *P*-values of comparisons between two groups were calculated using Student's *t*-test. Embryo developing beyond two-cell stage was the dichotomous dependent variable and Pifithrin-α treatment was covariates in the model using binary logistic repression analysis of SPSS software. $P < 0.05$ was considered as significant.

Acknowledgements

We thank Shiwen Li (Institute of Zoology, Chinese Academy of Sciences) for technical assistance and members of Li's laboratory for discussions and critical comments on the manuscript.

Competing interests

The authors declare no competing or financial interests.

Author contributions

Q.X. designed and performed the major experiments, analysed the data and wrote the manuscript. F.W. established the *Bcas2* transgenic mouse line and analysed its major phenotypes. Y.X. performed the microinjections. X.Z., Z.-A.Z., Z.G., W.L., X.L., Y.L., and X.-J.Y. contributed to mouse maintenance, embryo isolation and vector construction. H.W., J.H. and Z.Y. analysed the data. S.G. and L.L. initiated, organised and designed the study, analysed the data and wrote the manuscript. All authors commented on the manuscript.

Funding

The work was funded by the National Natural Science Foundation of China [31171382], the National Basic Research Program of China [2012CB944401, 2011CB944501] and the Strategic Priority Research Program of the Chinese Academy of Sciences [XDA01010103].

Supplementary information

Supplementary information available online at
http://dev.biologists.org/lookup/suppl/doi:10.1242/dev.129841/-/DC1

References

Abe, K.-I., Yamamoto, R., Franke, V., Cao, M., Suzuki, Y., Suzuki, M. G., Vlahovicek, K., Svoboda, P., Schultz, R. M. and Aoki, F. (2015). The first murine zygotic transcription is promiscuous and uncoupled from splicing and 3′ processing. *EMBO J.* **34**, 1523-1537.

Adiga, S. K., Toyoshima, M., Shiraishi, K., Shimura, T., Takeda, J., Taga, M., Nagai, H., Kumar, P. and Niwa, O. (2007). p21 provides stage specific DNA damage control to preimplantation embryos. *Oncogene* **26**, 6141-6149.

Ajuh, P., Kuster, B., Panov, K., Zomerdijk, J. C. B. M., Mann, M. and Lamond, A. I. (2000). Functional analysis of the human CDC5L complex and identification of its components by mass spectrometry. *EMBO J.* **19**, 6569-6581.

Anantha, R. W., Vassin, V. M. and Borowiec, J. A. (2007). Sequential and synergistic modification of human RPA stimulates chromosomal DNA repair. *J. Biol. Chem.* **282**, 35910-35923.

Anciano Granadillo, V. J., Earley, J. N., Shuck, S. C., Georgiadis, M. M., Fitch, R. W. and Turchi, J. J. (2010). Targeting the OB-folds of replication protein A with small molecules. *J. Nucleic Acids* **2010**, 304035.

Arias-Lopez, C., Lazaro-Trueba, I., Kerr, P., Lord, C. J., Dexter, T., Iravani, M., Ashworth, A. and Silva, A. (2006). P53 modulates homologous recombination by transcriptional regulation of the RAD51 gene. *EMBO Rep.* **7**, 219-224.

Artus, J. and Cohen-Tannoudji, M. (2008). Cell cycle regulation during early mouse embryogenesis. *Mol. Cell. Endocrinol.* **282**, 78-86.

Ashley, A. K., Shrivastav, M., Nie, J., Amerin, C., Troksa, K., Glanzer, J. G., Liu, S., Opiyo, S. O., Dimitrova, D. D., Le, P. et al. (2014). DNA-PK phosphorylation of RPA32 Ser4/Ser8 regulates replication stress checkpoint activation, fork restart, homologous recombination and mitotic catastrophe. *DNA Repair* **21**, 131-139.

Block, W. D., Yu, Y. and Lees-Miller, S. P. (2004). Phosphatidyl inositol 3-kinase-like serine/threonine protein kinases (PIKKs) are required for DNA damage-induced phosphorylation of the 32 kDa subunit of replication protein A at threonine 21. *Nucleic Acids Res.* **32**, 997-1005.

Bradley, M. O. and Taylor, V. I. (1981). DNA double-strand breaks induced in normal human cells during the repair of ultraviolet light damage. *Proc. Natl. Acad. Sci. USA* **78**, 3619-3623.

Brandriff, B. and Pedersen, R. A. (1981). Repair of the ultraviolet-irradiated male genome in fertilized mouse eggs. *Science* **211**, 1431-1433.

Brown, E. J. and Baltimore, D. (2000). ATR disruption leads to chromosomal fragmentation and early embryonic lethality. *Genes Dev.* **14**, 397-402.

Brugarolas, J., Chandrasekaran, C., Gordon, J. I., Beach, D., Jacks, T. and Hannon, G. J. (1995). Radiation-induced cell-cycle arrest compromised by P21 deficiency. *Nature* **377**, 552-557.

Bultman, S. J., Gebuhr, T. C., Pan, H., Svoboda, P., Schultz, R. M. and Magnuson, T. (2006). Maternal BRG1 regulates zygotic genome activation in the mouse. *Genes Dev.* **20**, 1744-1754.

Ciccia, A. and Elledge, S. J. (2010). The DNA damage response: making it safe to play with knives. *Mol. Cell* **40**, 179-204.

El-Deiry, W. S., Kern, S. E., Pietenpol, J. A., Kinzler, K. W. and Vogelstein, B. (1992). Definition of a consensus binding site for P53. *Nat. Genet.* **1**, 45-49.
Espinosa, J. M., Verdun, R. E. and Emerson, B. M. (2003). P53 functions through stress- and promoter-specific recruitment of transcription initiation components before and after DNA damage. *Mol. Cell* **12**, 1015-1027.
Fanning, E., Klimovich, V. and Nager, A. R. (2006). A dynamic model for Replication Protein A (RPA) function in DNA processing pathways. *Nucleic Acids Res.* **34**, 4126-4137.
Ferreira, J. and Carmo-Fonseca, M. (1997). Genome replication in early mouse embryos follows a defined temporal and spatial order. *J. Cell Sci.* **110**, 889-897.
Fraser, L. R. and Drury, L. M. (1975). Relationship between sperm concentration and fertilization in vitro of mouse eggs. *Biol. Reprod.* **13**, 513-518.
Friedberg, E. C. and Meira, L. B. (2006). Database of mouse strains carrying targeted mutations in genes affecting biological responses to DNA damage Version 7. *DNA Repair* **5**, 189-209.
Generoso, W. M., Cain, K. T., Krishna, M. and Huff, S. W. (1979). Genetic lesions induced by chemicals in spermatozoa and spermatids of mice are repaired in the egg. *Proc. Natl. Acad. Sci. USA* **76**, 435-437.
Goto, H., Tomono, Y., Ajiro, K., Kosako, H., Fujita, M., Sakurai, M., Okawa, K., Iwamatsu, A., Okigaki, T., Takahashi, T. et al. (1999). Identification of a novel phosphorylation site on histone H3 coupled with mitotic chromosome condensation. *J. Biol. Chem.* **274**, 25543-25549.
Grinfeld, S. and Jacquet, P. (1987). An unusual radiation-induced G2 arrest in the zygote of the BALB/c mouse strain. *Int. J. Radiat. Biol.* **51**, 353-363.
Hajkova, P., Jeffries, S. J., Lee, C., Miller, N., Jackson, S. P. and Surani, M. A. (2010). Genome-wide reprogramming in the mouse germ line entails the base excision repair pathway. *Science* **329**, 78-82.
Jazayeri, A., Falck, J., Lukas, C., Bartek, J., Smith, G. C. M., Lukas, J. and Jackson, S. P. (2006). ATM- and cell cycle-dependent regulation of ATR in response to DNA double-strand breaks. *Nat. Cell Biol.* **8**, 37-45.
Kojima, Y., Tam, O. H. and Tam, P. P. L. (2014). Timing of developmental events in the early mouse embryo. *Semin. Cell Dev. Biol.* **34**, 65-75.
Kuo, P.-C., Tsao, Y.-P., Chang, H.-W., Chen, P.-H., Huang, C.-W., Lin, S.-T., Weng, Y.-T., Tsai, T.-C., Shieh, S.-Y. and Chen, S.-L. (2009). Breast cancer amplified sequence 2, a novel negative regulator of the p53 tumor suppressor. *Cancer Res.* **69**, 8877-8885.
Larson, J. S., Stringer, S. L. and Stringer, J. R. (2004). Impact of mismatch repair deficiency on genomic stability in the maternal germline and during early embryonic development. *Mutat. Res.* **556**, 45-53.
Levine, A. J. (1997). p53, the cellular gatekeeper for growth and division. *Cell* **88**, 323-331.
Lewandoski, M., Wassarman, K. M. and Martin, G. R. (1997). Zp3-cre, a transgenic mouse line for the activation or inactivation of loxP-flanked target genes specifically in the female germ line. *Curr. Biol.* **7**, 148-151.
Li, L., Zheng, P. and Dean, J. (2010). Maternal control of early mouse development. *Development* **137**, 859-870.
Liu, Q. H., Guntuku, S., Cui, X. S., Matsuoka, S., Cortez, D., Tamai, K., Luo, G. B., Carattini-Rivera, S., DeMayo, F., Bradley, A. et al. (2000). Chk1 is an essential kinase that is regulated by Atr and required for the G(2)/M DNA damage checkpoint. *Genes Dev.* **14**, 1448-1459.
Liu, S., Opiyo, S. O., Manthey, K., Glanzer, J. G., Ashley, A. K., Amerin, C., Troksa, K., Shrivastav, M., Nickoloff, J. A. and Oakley, G. G. (2012). Distinct roles for DNA-PK, ATM and ATR in RPA phosphorylation and checkpoint activation in response to replication stress. *Nucleic Acids Res.* **40**, 10780-10794.
Luo, G., Yao, M. S., Bender, C. F., Mills, M., Bladl, A. R., Bradley, A. and Petrini, J. H. J. (1999). Disruption of mRad50 causes embryonic stem cell lethality, abnormal embryonic development, and sensitivity to ionizing radiation. *Proc. Natl. Acad. Sci. USA* **96**, 7376-7381.
Macleod, K. F., Sherry, N., Hannon, G., Beach, D., Tokino, T., Kinzler, K., Vogelstein, B. and Jacks, T. (1995). P53-dependent and independent expression of P21 during cell growth, differentiation, and DNA damage. *Genes Dev.* **9**, 935-944.
Marangos, P. and Carroll, J. (2012). Oocytes progress beyond prophase in the presence of DNA damage. *Curr. Biol.* **22**, 989-994.
Maréchal, A., Li, J.-M., Ji, X. Y., Wu, C.-S., Yazinski, S. A., Nguyen, H. D., Liu, S., Jiménez, A. E., Jin, J. and Zou, L. (2014). PRP19 transforms into a sensor of RPA-ssDNA after DNA damage and drives ATR activation via a ubiquitin-mediated circuitry. *Mol. Cell* **53**, 235-246.
Masui, Y. and Pedersen, R. A. (1975). Ultraviolet light-induced unscheduled DNA synthesis in mouse oocytes during meiotic maturation. *Nature* **257**, 705-706.
Miyashita, T. and Reed, J. C. (1995). Tumor suppressor P53 is a direct transcriptional activator of the human Bax gene. *Cell* **80**, 293-299.
Nagasaki, K., Maass, N., Manabe, T., Hanzawa, H., Tsukada, T., Kikuchi, K. and Yamaguchi, K. (1999). Identification of a novel gene, DAM1, amplified at chromosome 1p13.3-21 region in human breast cancer cell lines. *Cancer Lett.* **140**, 219-226.
Oakley, G. G., Patrick, S. M., Yao, J., Carty, M. P., Turchi, J. J. and Dixon, K. (2003). RPA phosphorylation in mitosis alters DNA binding and protein-protein Interactions. *Biochemistry* **42**, 3255-3264.
O'Connell, M. J., Raleigh, J. M., Verkade, H. M. and Nurse, P. (1997). Chk1 is a wee1 kinase in the G(2) DNA damage checkpoint inhibiting cdc2 by Y15 phosphorylation. *EMBO J.* **16**, 545-554.
O'Driscoll, M. and Jeggo, P. A. (2006). The role of double-strand break repair - insights from human genetics. *Nat. Rev. Genet.* **7**, 45-54.
Olson, E., Nievera, C. J., Klimovich, V., Fanning, E. and Wu, X. (2006). RPA2 is a direct downstream target for ATR to regulate the S-phase checkpoint. *J. Biol. Chem.* **281**, 39517-39533.
Posfai, E., Kunzmann, R., Brochard, V., Salvaing, J., Cabuy, E., Roloff, T. C., Liu, Z., Tardat, M., van Lohuizen, M., Vidal, M. et al. (2012). Polycomb function during oogenesis is required for mouse embryonic development. *Genes Dev.* **26**, 920-932.
Rodriguez, C. I., Buchholz, F., Galloway, J., Sequerra, R., Kasper, J., Ayala, R., Stewart, A. F. and Dymecki, S. M. (2000). High-efficiency deleter mice show that FLPe is an alternative to Cre-loxP. *Nat. Genet.* **25**, 139-140.
Roest, H. P., Baarends, W. M., de Wit, J., van Klaveren, J. W., Wassenaar, E., Hoogerbrugge, J. W., van Cappellen, W. A., Hoeijmakers, J. H. J. and Grootegoed, J. A. (2004). The ubiquitin-conjugating DNA repair enzyme HR6A is a maternal factor essential for early embryonic development in mice. *Mol. Cell. Biol.* **24**, 5485-5495.
Sanchez, Y., Wong, C., Thoma, R. S., Richman, R., Wu, Z., Piwnica-Worms, H. and Elledge, S. J. (1997). Conservation of the Chk1 checkpoint pathway in mammals: linkage of DNA damage to Cdk regulation through Cdc25. *Science* **277**, 1497-1501.
Shi, W., Feng, Z., Zhang, J., Gonzalez-Suarez, I., Vanderwaal, R. P., Wu, X., Powell, S. N., Roti, J. L. R., Gonzalo, S. and Zhang, J. (2010). The role of RPA2 phosphorylation in homologous recombination in response to replication arrest. *Carcinogenesis* **31**, 994-1002.
Shiloh, Y. (2001). ATM and ATR: networking cellular responses to DNA damage. *Curr. Opin. Genet. Dev.* **11**, 71-77.
Shuck, S. C. and Turchi, J. J. (2010). Targeted inhibition of Replication Protein A reveals cytotoxic activity, synergy with chemotherapeutic DNA-damaging agents, and insight into cellular function. *Cancer Res.* **70**, 3189-3198.
Siafakas, A. R. and Richardson, D. R. (2009). Growth arrest and DNA damage-45 alpha (GADD45 alpha). *Int. J. Biochem. Cell Biol.* **41**, 986-989.
Takai, H., Tominaga, K., Motoyama, N., Minamishima, Y. A., Nagahama, H., Tsukiyama, T., Ikeda, K., Nakayama, K., Nakanishi, M. and Nakayama, K. (2000). Aberrant cell cycle checkpoint function and early embryonic death in Chk1 (-/-) mice. *Genes Dev.* **14**, 1439-1447.
Toyoshima, M., Shimura, T., Adiga, S.-K., Taga, M., Shiraishi, K., Inoue, M., Yuan, Z.-M. and Niwa, O. (2005). Transcription-independent suppression of DNA synthesis by p53 in sperm-irradiated mouse zygotes. *Oncogene* **24**, 3229-3235.
Wan, L. and Huang, J. (2014). The PSO4 protein complex associates with Replication Protein A (RPA) and modulates the activation of Ataxia Telangiectasia-mutated and Rad3-related (ATR). *J. Biol. Chem.* **289**, 6619-6626.
Wang, H. Y., Guan, J., Wang, H. C., Perrault, A. R., Wang, Y. and Iliakis, G. (2001). Replication protein A2 phosphorylation after DNA damage by the coordinated action of ataxia telangiectasia-mutated and DNA-dependent protein kinase. *Cancer Res.* **61**, 8554-8563.
Wang, Y., Putnam, C. D., Kane, M. F., Zhang, W., Edelmann, L., Russell, R., Carrión, D. V., Chin, L., Kucherlapati, R., Kolodner, R. D. et al. (2005). Mutation in Rpa1 results in defective DNA double-strand break repair, chromosomal instability and cancer in mice. *Nat. Genet.* **37**, 750-755.
Wossidlo, M., Arand, J., Sebastiano, V., Lepikhov, K., Boiani, M., Reinhardt, R., Schöler, H. and Walter, J. (2010). Dynamic link of DNA demethylation, DNA strand breaks and repair in mouse zygotes. *EMBO J.* **29**, 1877-1888.
Wu, X., Viveiros, M. M., Eppig, J. J., Bai, Y., Fitzpatrick, S. L. and Matzuk, M. M. (2003). Zygote arrest 1 (Zar1) is a novel maternal-effect gene critical for the oocyte-to-embryo transition. *Nat. Genet.* **33**, 187-191.
Zeng, F. and Schultz, R. M. (2005). RNA transcript profiling during zygotic gene activation in the preimplantation mouse embryo. *Dev. Biol.* **283**, 40-57.
Zeng, F., Baldwin, D. A. and Schultz, R. M. (2004). Transcript profiling during preimplantation mouse development. *Dev. Biol.* **272**, 483-496.
Zou, L. and Elledge, S. J. (2003). Sensing DNA damage through ATRIP recognition of RPA-ssDNA complexes. *Science* **300**, 1542-1548.

Supplemental figures Legends, tables and figures

Xu et al.,

Maternal BCAS2 protects genomic integrity through RPA in mouse preimplantation embryos

Qianhua Xu[1,2,7], Fengchao Wang[3,7], Yunlong Xiang[1], Xiaoxin Zhang[1], Zhenao Zhao[1], Zheng Gao[1,2], Wenbo Liu[1], Xukun Lu[1,2], Yusheng Liu[1], Xing-jiang Yu[1], Haibin Wang[1], Jun Huang[4], Zhaohong Yi[5], Shaorong Gao[6,8], Lei Li[1,8]

[1]State Key Laboratory of Stem Cell and Reproductive Biology, Institute of Zoology, Chinese Academy of Sciences, Beijing, 100101, China. [2]University of Chinese Academy of Sciences, Beijing, 100049, China. [3]National Institute of Biological Sciences, Beijing, 102206, China. [4]Life Sciences Institute, Zhejiang University, Hangzhou, Zhejiang, 310058, China. [5]College of Biological Science and Engineering, Beijing University of Agriculture, Beijing, 102206, China. [6]School of Life Sciences and Technology, Tongji University, Shanghai, 200092, China.

Figure S1

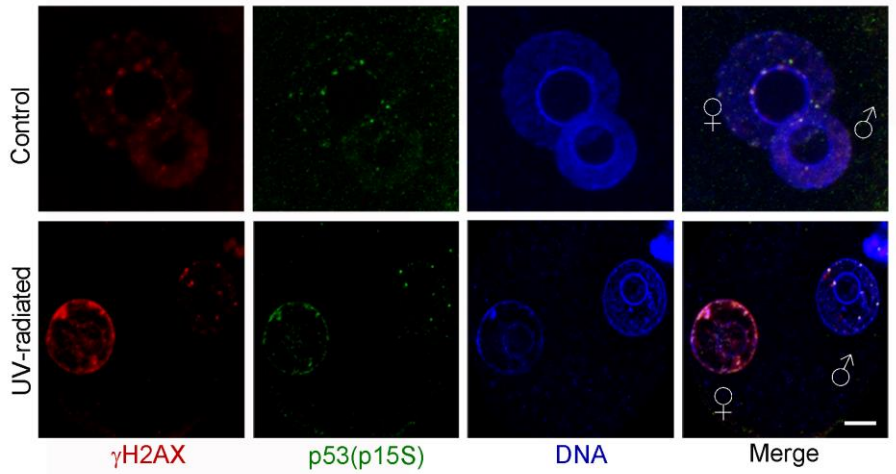

Fig. S1. BCAS2 responses to UV-induced DNA damage. MII oocytes were UV-irradiated and *in vitro* fertilized with normal sperms. Zygotes were cultured until PN4-5 and immunostained with phosphor-p53 (p15S) and γH2AX. Male- and female pronuclei are indicated with male and female symbols, respectively. Scale bar, 10 μm.

Figure S2

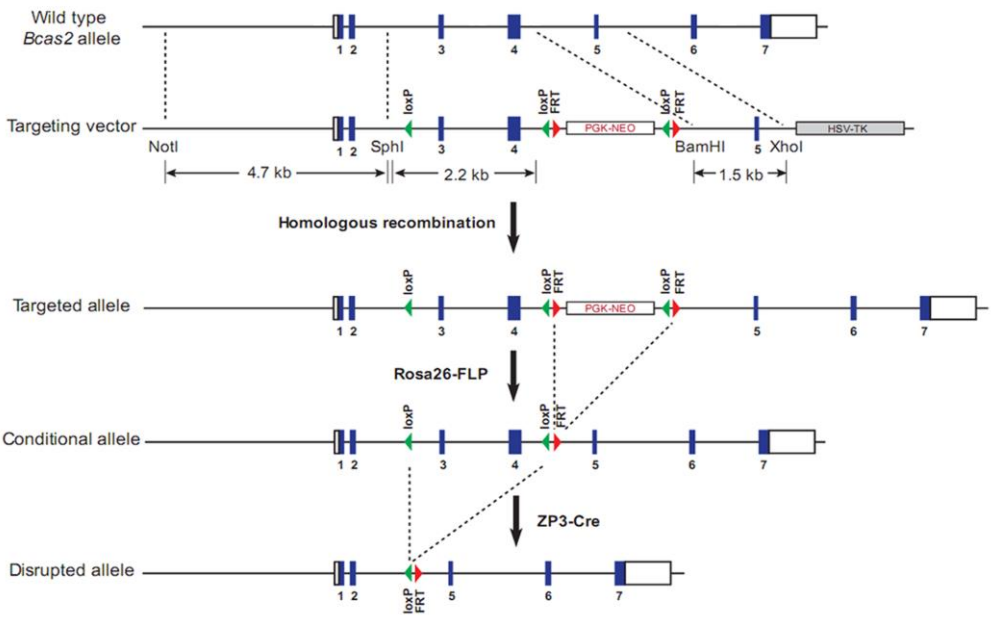

Fig. S2. *Bcas2* targeting strategy and analysis of F2 offspring. A targeting vector was constructed by anchoring LoxP sites around exon 3 and exon 4. HSV-TK expression was used for negative selection, and PGK-NEO expression was used for positive selection. Targeted ES clones were confirmed by sequencing and injected into blastocysts to produce chimeric mice.

Figure S3

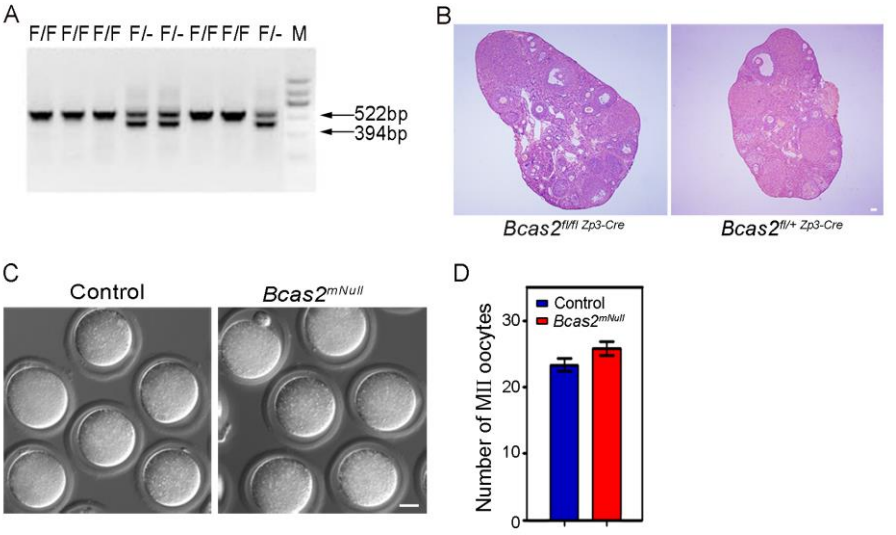

Fig. S3. Characterization of *Bcas2$^{fl/fl}$* and *Bcas2$^{fl/fl}$;Zp3-Cre* mice. (A) PCR analysis of genomic DNA derived from eight offspring. (B) Ovaries from two-month old *Bcas2$^{fl/+}$;Zp3-Cre* and *Bcas2$^{fl/fl}$;Zp3-Cre* females were fixed and stained with hematoxylin and eosin. Scale bar, 50 μm. (C and D) MII oocytes were obtained from *Bcas2$^{fl/+}$;Zp3-Cre* and *Bcas2$^{fl/fl}$;Zp3-Cre* females after 13 hours post-hCG. Scale bar, 20 μm.

Figure S4

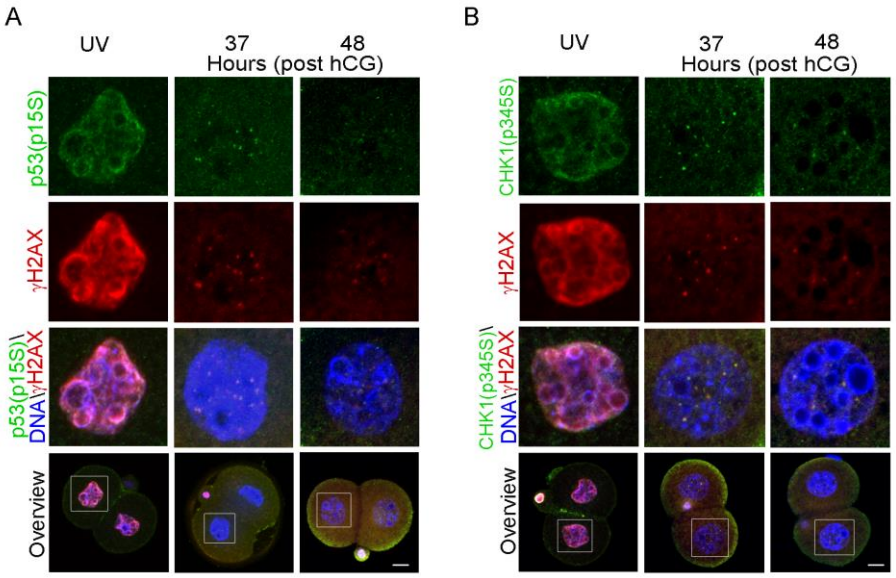

Fig. S4. Checkpoint activation during cell cycle progression in normal two-cell embryos. (A) Normal two-cell embryos at 37 and 48 hrs post-hCG were fixed and stained with γH2AX and phosphor-p53 (S15) antibodies under TP conditions. (B) Normal two-cell embryos at 37 and 48 hours post-hCG were fixed and stained with γH2AX and phosphor-pCHK1(S345) antibodies under TP conditions. Normal two-cell embryos irradiated by UV were positive control. Scale bar, 20 μm.

Figure S5

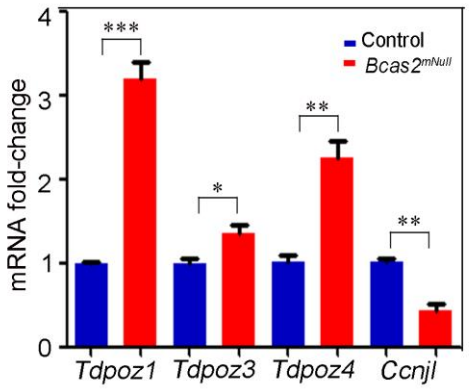

Fig. S5. Zygotic genome active is partially impaired in *Bcas2*^{mNull} two-cell embryos. Levels of *Tdpoz1, Tdpoz3, Tdpoz4, Ccnjl* and *Gm13043* were measured by qRT-PCR with specific primers (Table S 4) in two-cell embryos obtained at 48 hrs post-hCG. The error bars represent the SEM from three independent experiments. *, $P < 0.05$; **, $P < 0.01$; ***, $P< 0.001$.

Figure S6

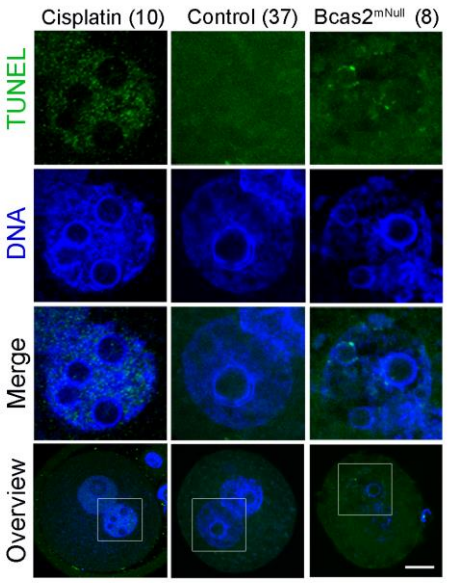

Fig. S6. BCAS2 is required for DNA repair in mouse zygotes. Control and BCAS2^{mNull} zygotes were obtained 30 hrs post-hCG and examined by TUNEL assay. Normal zygotes treated with Casplatin as the positive control.

Figure S7

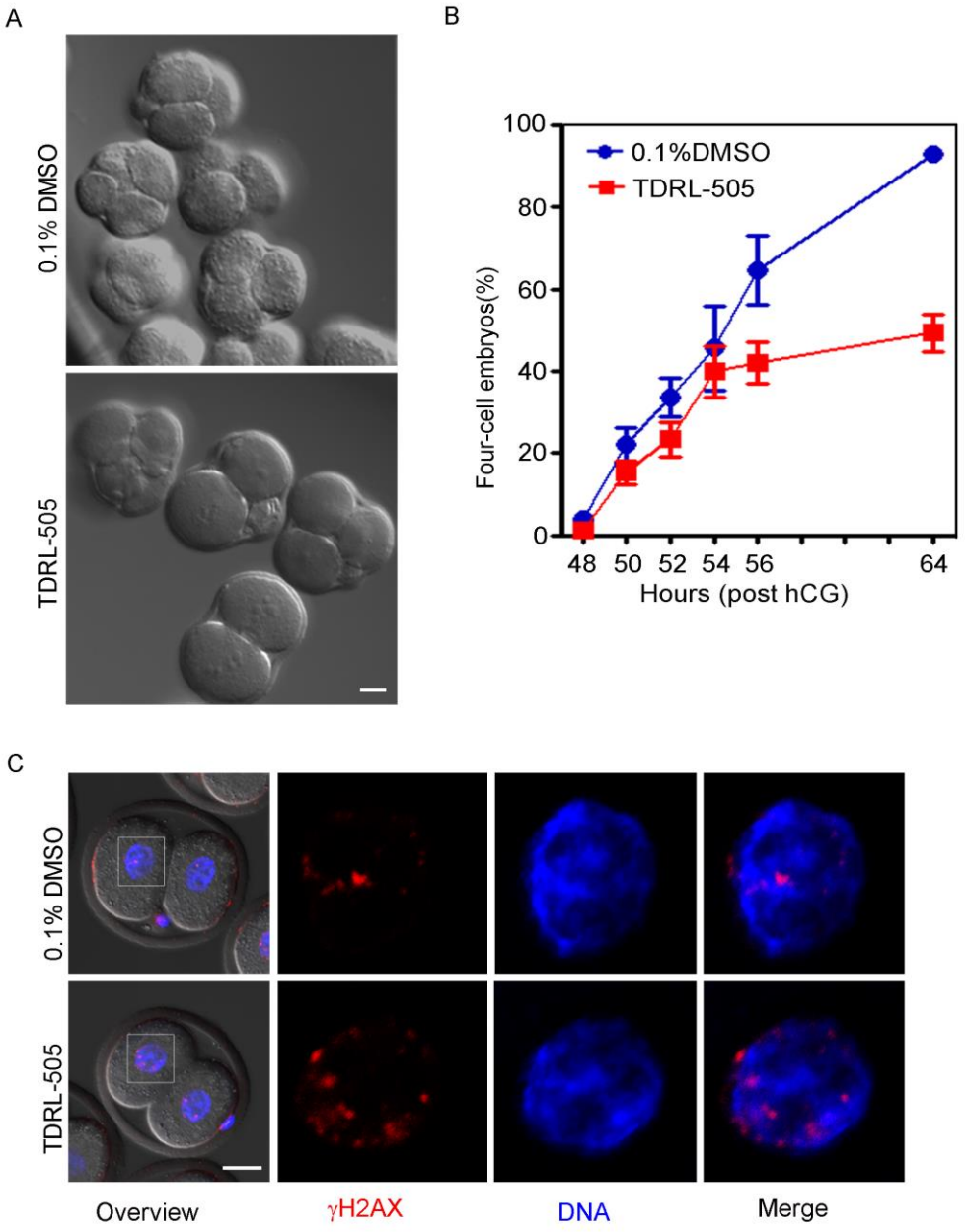

Fig. S7. RPA inhibition induces developmental arrest and increased γH2AX at two-cell stage. (A) Normal zygotes were recovered 23 hrs post-hCG. Zygotes were treated with either 0.1% DMSO as control (n=65) or 100 μM TDRL-505 (n=68) for 5 hrs and released. Zygotes were allowed to progress to the four-cell stage. (B) Quantification of (A) developmental rate

during the transition from the two- to four-cell stage. Developmental rates were calculated without the amount of arrested two-cell embryos. Error bars represented SEM. (C) Two-cell embryos from (B) were fixed after 48 hours post-hCG and immunostained with γH2AX. Scale bar, 20 μm.

Supplementary Table S1

PCR primers used for gene targeting at Bcas2 locus and genotyping.

Primer	5'->3'
SphI-Loxp-F	ACAGCATGCATAACTTCGTATAGCATACATTATACGAAG TTATGTTTTTAAGTGGTTATTCTACAAGTGC
NotI-R	GAATTCGCGGCCGCTGTAGTTCTGAGACAATCCC
Not-F	GAATTCGCGGCCGCGTGCCAACGACAGTGTTTTC
SphI-R:	ACAGCATGCAGTTAGACATGCTTGTTCAGGC
BamHI-F:	TCGGATCCCAACGAAAGGCTACCTTGAG
XhoI-R:	TCCTCGAGCTAACTGTGAAGGTGTGTCAG
Neo-F:	TATCGCCTTCTTGACGAGTTC
screen-R	TTGGTCCTGCAGTCCAAATC
F-WT	ATTCCAGCAGTTGGTGTGGG
F2-KO	AGGTGTATGAATGCCTGAACAAG
R	CATTGCTGGACAGAAGGTGAG

Supplementary Table S2

Antibodies used in this study:

Name	Dilution	Application
anti-BCAS2 (Protein Tech Group, 10414)	IF	1: 200
	WB	1:600
anti-phosphor-p53 on Ser15 (Cell Signaling, 9284)	IF	1:100
	WB	1:1000
anti-γH2AX antibody (Cell signaling, 22551)	IF	1: 500
	WB	1:1000
phosphor-RPA2 (Bethyl Laboratories, A300-245A)	IF	1:100
anti-β-Actin monoclonal antibody (ZSGB-BIO, ZM0002)	WB	1: 5000
Alexa 488 donkey anti-rabbit (Jackson, 711545152)	IF	1:1000
Alexa 633 donkey anti-mouse (Jackson, A-21050)	IF	1:200
HRP-conjugated anti-mouse (ZSGB-BIO; 2304)	WB	1:5000
HRP-conjugated anti-rabbit secondary antibodies (ZSGB-BIO; 2301)	WB	1:5000

Abbreviation: IF, immunofluorescence staining; WB, western blotting.

SupplementaryTable S3

Primer sequences for *Bcas2* and *Rpa2* mutations:

Gene	Forward (5'->3')	Reverse (5'->3')
Bcas2	TAGAATTCGCCACCATGGGGGCACGGGCTTGGTAGCCGGAGAGG	TACCGCGGGAAGTCTTGGCGGATGTTTTCCTTGTTGGCCTCCC
ΔN	GAATTCGCCACCATGGCGGCACGGGCTTGGT	TTGACCGCGGTCATTCTCTCAGCTTAGATC
Rpa2	TGCGGATATCATGTGGAATAGCGGATTCGA	AGGAGGCGCGCCTCACTCTGCATCTGTAGACT
Rpa2(S4A/S8A)	AGGTGGAGCTGCTGAAGCCTTCGAATCCGCCATTCCACAT	ATGTGGAATGGCGGATTCGAAGGCTTCAGCAGCTCCACCT
Rpa2(S33A)	CTCGATTTCTTCTCCGCCTGCGCCGGTGTGGGCGACCCGA	TCGGGTCGCCCACACCGGCGCAGGCGGAGAAGAAATCGAG
Rpa2(Thr21A)	CCGAAGCCACCGGGGGACTGCGCGTAGCCGCCTGCTCCGCC	GGCGGAGCAGGCGGCTACGCGCAGTCCCCCGGTGGCTTCGG

Supplementary Table S4

Primers for qRT-PCR assay:

Gene	Forward (5'->3')	Reverse (5'->3')
Bcas2	5'TCGCTGCTCGACAACCGATTGAA3'	5'AGCTGCATGTTCTTTCGCTGCCA3'
P21	5'GCAGCCGAGAGGTGTGAGCC3'	5'CGGGACCGAAGAGACAACGGC3'
Gadd45a	CTGCAGAGCAGAAGACCGAA	TACACGCCGACCGTAATGG
Tdpoz1	TCAGAGAAGGATTACAAGCCCA	GGCTGAGCAAAACTAGGTAAACT
Tdpoz3	CCTGTCAGTTTATCTGGAGTTGC	CAGAAAGCATTGGACATTGGAGA
Tdpoz4	GCCCAAGTGCTAACACCAGA	TCCCACAGCTCCCCTACGT
Ccnjl	TGGCATATCGGGACTCGTTG	ATATCCAAGGGCTGGAGGGT
Gm13043	GCCCCACTCTATCTGTTTTGC	AACGAATCCTCCTCCTATTTACTG